Marine Geology 430 (2020) 106356

Contents lists available at ScienceDirect

Marine Geology

journal homepage: www.elsevier.com/locate/margo

# Intermediate and deep ocean current circulation in the Mozambique Channel: New insights from ferromanganese crust Nd isotopes

Claire Charles [a,b,*], Ewan Pelleter [a], Sidonie Révillon [b,c], Philippe Nonnotte [b], Stephan J. Jorry [a], Jean-Michel Kluska [d]

[a] IFREMER, Unité Géosciences Marines, Laboratoire Cycles Géochimiques (LCG), F-29280 Plouzané, France
[b] Univ Brest, CNRS, UMR 6538 (Laboratoire Géosciences Océan), Institut Universitaire Européen de la Mer (IUEM), Place Nicolas Copernic, 29280 Plouzané, France
[c] SEDISOR/UMR 6538 (Laboratoire Géosciences Océan), Institut Universitaire Européen de la Mer (IUEM), Place Nicolas Copernic, F-29280 Plouzané, France
[d] TOTAL Exploration and Production, CSTJF, Avenue Larribau, F-64000, Pau, France

ARTICLE INFO

*Keywords:*
Ferromanganese crusts
Nd isotopes
Paleoceanography
Mozambique Channel
North Atlantic Deep Water

ABSTRACT

The Mozambique Channel plays a key role in the exchange of water masses between the Indian and Atlantic Oceans, which include the North Atlantic Deep Water (NADW) inflow from the south and the North Indian Deep Water (NIDW), an aged form of the NADW spreading poleward from the northern and equatorial Indian Ocean basin. Several authors assume that the Davie Ridge acts as a topographic barrier to the northward advection of NADW, which would therefore be absent in the Comoros Basin. Other studies suggest that the NADW flows from the south of the Mozambique Channel to the Comoros Basin, indicating that the Davie Ridge may not currently constitute a blocking topographic barrier to deep water mass circulation. To address this question, we studied ferromanganese (Fe, Mn) crusts collected over 2000 km in the Mozambique Channel, from the Agulhas Plateau to the Glorieuses Islands. Neodymium (Nd) isotope compositions ($\varepsilon_{Nd}$) of surface scrapings range between $\varepsilon_{Nd} = -10.1$ above the Agulhas Plateau, which might reflect the NADW inflow, and more radiogenic values between $\varepsilon_{Nd} = -8.0$ and $-8.2$ in the Glorieuses area, highlighting the NIDW influence. However, value of $\varepsilon_{Nd} = -9.4$ measured north of the Davie Ridge cannot be explained by the sole influence of the NIDW and therefore highlights the advection of the NADW northeast of the Comoros Basin. We estimate that the contribution of the NADW through the channel is up to 68% in the Agulhas Plateau and 60% north of the Davie Ridge. These findings are consistent with previous hydrographic studies and suggest that the Davie Ridge does not currently act as topographic barrier to deep currents.

## 1. Introduction

Ferromanganese crusts (Fe, Mn) are marine deposits that are ubiquitous on the seafloor i.e. occur in diverse environments and at different depths. They precipitate directly from seawater on hard substrates (Hein et al., 2009) and their growth rate can vary between 0.5 and 15 mm/Ma according to the geodynamic and paleogeographic context (Kusakabe and Ku, 1984; Segl et al., 1984; Eisenhauer et al., 1992; Frank et al., 1999). As a result, the thickest crusts may represent time intervals up to 80 Ma (Frank et al., 1999). This very low precipitation rate, coupled with the fact that Fe and Mn oxyhydroxides are significant element scavengers (e.g. metals, trace elements, rare earth elements (REE); Piper, 1974; Hein et al., 2010; Lusty et al., 2018), results over time in extensive enrichment of seawater elements in the Fe-Mn crusts. These crusts therefore contain records of element cycles in the oceans (Aplin and Cronan, 1985) with each millimeter of thickness corresponding to a specific time period. They constitute ocean archives, studied since the 1980s to understand the biogeochemical cycles of metals (Koschinsky and Halbach, 1995; Koschinsky et al., 1997), and more recently, to trace global ocean current flow paths (Albarède and Goldstein, 1992; Albarède et al., 1997; Christensen et al., 1997; Frank et al., 1999). Several authors have focused on multi-element and isotopic compositions of Fe-Mn crusts from the Atlantic, Indian and Pacific Oceans. Their neodymium (Nd) isotope compositions ($\varepsilon_{Nd}$) have been particularly assessed (Aplin et al., 1986; Albarède et al., 1997, 1998; Frank et al., 1999). These previous global-scale studies have established the current average geochemical compositions of seawater for each geographic oceanic basin and identified major geodynamic, geochemical and

* Corresponding author.
*E-mail address:* claire.charles@ifremer.fr (C. Charles).

https://doi.org/10.1016/j.margeo.2020.106356
Received 5 April 2020; Received in revised form 10 August 2020; Accepted 23 September 2020
Available online 28 September 2020

climate changes over the past 15 Ma (Segl et al., 1984; Christensen et al., 1997; Ling et al., 1997; Frank and O'Nions, 1998; O'Nions et al., 1998; Frank et al., 1999; Frank et al., 2002; Hein et al., 2016). However, few analyses have been made on Fe-Mn crusts on local scale in mixing areas such as the Mozambique Channel, a strategic zone for studying the Atlantic and Indian water mass mixing (You, 2000; de Ruijter et al., 2002; van Aken et al., 2004; Collins et al., 2016; Fig. 1).

The circulation of deep currents is widely described due to the Davie Ridge (Coffin and Rabinowitz, 1987) that separates the channel into two distinct basins (i.e. the Comoros Basin in the north and the Mozambique Basin in the south; Fig. 1). According to some authors, the Davie Ridge represents a topographic obstacle to the circulation of these deep currents flowing from the Atlantic Ocean to the south and from the Indian Ocean to the north (Toole and Warren, 1993; Mantyla and Reid, 1995;

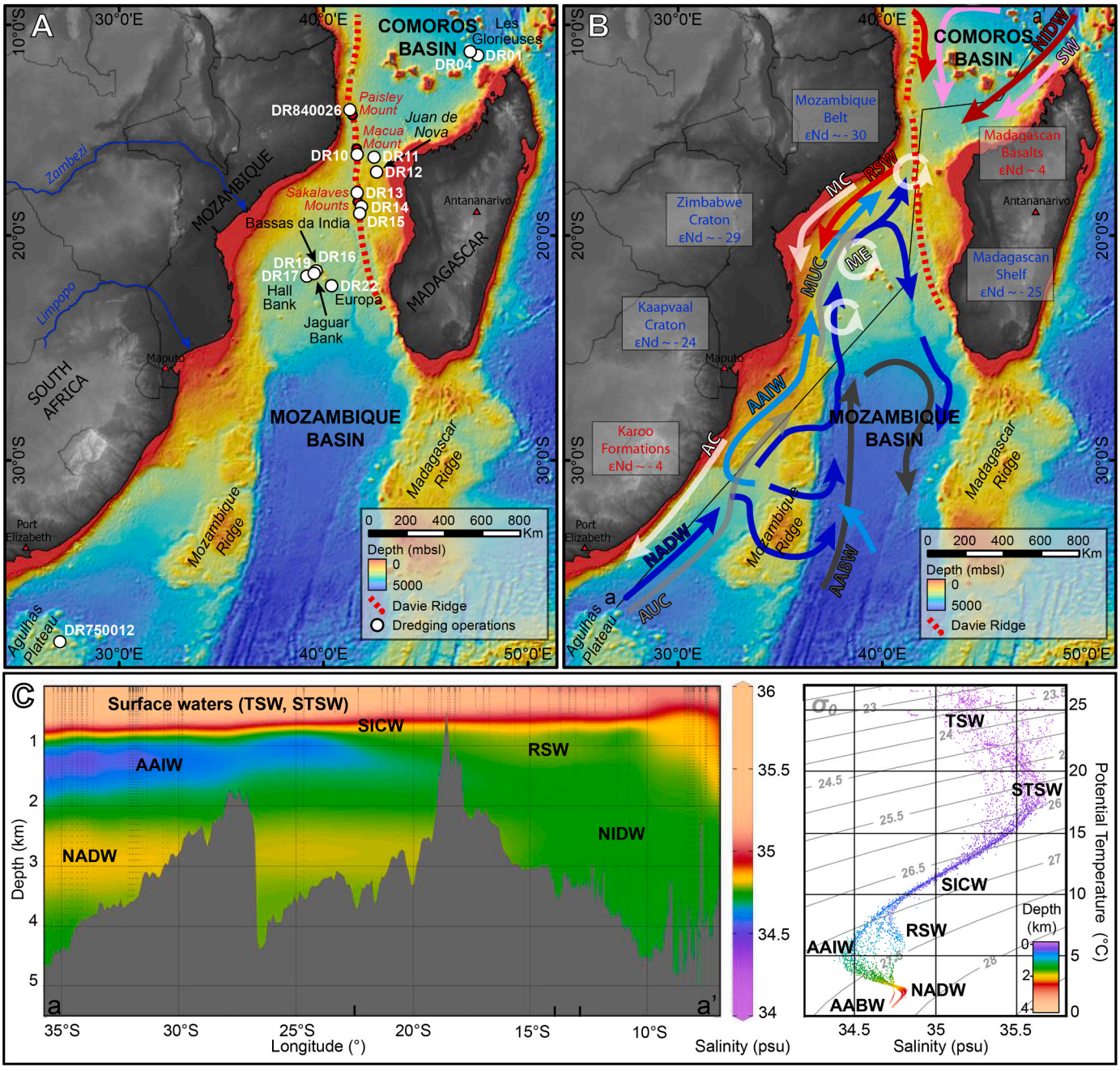


**Fig. 1.** (A) Bathymetry of the Mozambique Channel (data from GEBCO and PAMELA cruises) with its main structures including the Davie Ridge and the Eparses Islands. The white dots represent the dredging operations. (B) Bathymetry of the Mozambique Channel (data from GEBCO and PAMELA cruises) showing the main circulation patterns (based on Kolla et al., 1980; Fine, 1993; Toole and Warren, 1993; DiMarco et al., 2002; Lutjeharms, 2006; Ullgren et al., 2012). AABW: Antarctic Bottom Water; AAIW: Antarctic Intermediate Water; AC: Agulhas Current; AUC: Agulhas Undercurrent; MC: Mozambique Current; ME: Mozambique Eddies; MUC: Mozambique Undercurrent; NADW: North Atlantic Deep Water; NIDW: North Indian Deep Water; RSW: Red Sea Water; SW: Surface Water including TSW: Tropical Surface Water, STSW: Sub-Tropical Surface Water and SICW: South Indian Central Water. The dark line corresponds to the section located in 1C. Nd isotope signatures ($\varepsilon_{Nd}$) are presented for the main geological formations surrounding the channel ($\varepsilon_{Nd}$ of Archean basement: Paquette et al., 1994; Jelsma et al., 1996; Möller et al., 1998; Kröner et al., 2000; De Waele et al., 2006; Grantham et al., 2011 and $\varepsilon_{Nd}$ of the volcanic structures: Mahoney et al., 1991; Grousset et al., 1992; Jourdan et al., 2007). (C) Salinity section showing the distribution of the main water masses present in the Mozambique Channel, based on Conductivity Temperature Depth (CTD) profiles.

You, 2000; Fig. 1B). However, recent hydrographic data have identified deep currents from the Atlantic Ocean north of the Davie Ridge (DiMarco et al., 2002; van Aken et al., 2004; Collins et al., 2016), and thus called into question the evolution of deep currents in the Mozambique Channel as well as the role of the Davie Ridge in the distribution of these water masses.

In this study, we analyzed the Nd isotope composition of 29 crusts collected through the Mozambique Channel in order to better understand the oceanic processes in the study area. The main objectives of this paper are to (1) identify deep water masses circulation (2) interpret the actual impact of the Davie Ridge on water mass propagation to the north and (3) propose new hydrographic framework of the deep currents in the Mozambique Channel. This is the first time that such a detailed study in terms of the number of dredges and various water depths has been carried out and used for an oceanographic study on a regional scale.

## 2. Regional setting and geochemical approach

### 2.1. Geological setting

The Mozambique Channel is located in the southwestern Indian Ocean, between the East-African continental margin along Mozambique and Madagascar (Fig. 1A). It resulted from the separation of the eastern part (Madagascar, India, Antarctica and Australia) and the western part of Gondwana (Africa and South America) in the lower Jurassic (McElhinny, 1970; McKenzie and Sclater, 1971). The Antarctic-India-Madagascar structure was relocated southward along a major transform zone called the Davie Fracture Zone (DFZ) to the Upper Cretaceous (Heirtzler and Burroughs, 1971; Coffin and Rabinowitz, 1987; Gaina et al., 2013). This tectonic event is now represented by the Davie Ridge (Fig. 1A), oriented N170, which extends 1200 km east of the African continental margin (15°S) to the Madagascan marginal plateau (22°S). The ridge is punctuated by several seamounts (e.g. Paisley, Macua and Sakalaves) and separates the Comoros basin in the northeast from the deep Mozambique basin in the southwest (Fig. 1A). The major Jurassic structuring phase was followed by the separation of Madagascar and the Antarctic-India block in the Upper Cretaceous, which caused important volcanic activity in Madagascar but also in the Morondava and Majunga basins to the west of the island (Bassias, 1992; Storey et al., 1995; Rogers et al., 2000; Torsvik et al., 2000; Thompson et al., 2019; Fig. 1A). The Eparses Islands (Bassas Da India, Europa, Juan de Nova, and the Glorieuses Islands) have witnessed this volcanic activity since their formation in the Paleocene. Linked to these volcanic events, these islands and the northern part of the Madagascan continental margin are assigned a radiogenic Nd isotope signature of $\varepsilon_{Nd} \sim 4$ (Mahoney et al., 1991; Jeandel et al., 2007), whereas Madagascar presents an Archean signature in the center and in the south, characterized by an average unradiogenic value of $\varepsilon_{Nd} \sim -25$ (from $\varepsilon_{Nd} = -22$ to $\varepsilon_{Nd} = -28$; Paquette et al., 1994; Kröner et al., 2000; Fig. 1B). On the other side of the Mozambique channel, the African continental margin is assigned an unradiogenic value of $\varepsilon_{Nd} \sim -20$ (Jeandel et al., 2007). This may represent an average of Nd isotope signatures from old continental crustal sources as the Archean Kaapvaal craton ($\varepsilon_{Nd} \sim -24$; Grantham et al., 2011), Zimbabwe craton ($\varepsilon_{Nd} \sim -29$; Jelsma et al., 1996) and Mozambique belt ($\varepsilon_{Nd} \sim -30$; Möller et al., 1998; Fig. 1B) and, younger volcanic sources as the Jurassic Karoo formations with more radiogenic signature of $\varepsilon_{Nd} \sim -4$ (from $\varepsilon_{Nd} = -9$ to $\varepsilon_{Nd} = 0$; Grousset et al., 1992; Jourdan et al., 2007; Fig. 1B).

### 2.2. Oceanic setting

The Mozambique Channel is a complex oceanic area with (1) exchange between the water masses of the Indian and Atlantic Oceans and (2) the Davie Ridge which constitutes a topographic high ranging from several tens to 100 km in width and characterized by a basement which culminates at 300 m below sea level (mbsl) and extends to 2500 mbsl (Mougenot et al., 1986; Coffin and Rabinowitz, 1987; Fig. 1C). This ridge separates the Mozambique Channel into distinct basins (Fig. 1A). Warm Indian water masses spread from the Comoros Basin and then are dragged into the Mozambique Current (MC) in the Deep Basin (DiMarco et al., 2002; Quartly et al., 2013; Flemming and Kudrass, 2018). The deep water flows in the Mozambique Undercurrent (MUC) from the south of the Mozambique Basin to the west of the ridge (de Ruijter et al., 2002; Fig. 1B).

The MC is part of the Agulhas Current (AC), which is an essential link for heat and salt exchanges between the Indian and Atlantic Oceans (Gordon, 1986; Weijer, 1999; Lutjeharms, 2006), and is characterized by anticyclonic eddies (ME) up to 300 km in diameter that can affect the entire water column (de Ruijter et al., 2002; Halo et al., 2014; Fig. 1B). The MC transports surface water to a depth of 600 mbsl, composed of Tropical Surface Water (TSW) and Subtropical Surface Water (STSW) but also South Indian Central Water (SICW) between 200 and 600 mbsl (Fig. 1C). The intermediate waters of the MC are composed of Red Sea Water (RSW) between 900 and 1200 mbsl that enters from the north of the Mozambique Channel along the East African coast (Beal et al., 2000; Schott and McCreary, 2001; Fig. 1B, C).

The MUC and the Agulhas Undercurrent (AUC) carry Antarctic Intermediate Water (AAIW) between 800 and 1500 mbsl (Ullgren et al., 2012; Fig. 1B, C). AAIW arrives from the eastern part of the Mozambique ridge and then flows along the Mozambican coast (Fine, 1993). The North Atlantic Deep Water (NADW) is also part of the MUC, between 1500 and 3500 mbsl (Fig. 1B, C). Its inflow starts upstream of the south of Africa before entering the Mozambique Channel through the Natal Valley (Toole and Warren, 1993). The NADW flows northwards from the Mozambique Basin to the west of the Davie Ridge. Several authors consider that this water mass does not flow over the Davie Ridge and retreats south along the western edge of the ridge (Toole and Warren, 1993; Mantyla and Reid, 1995; You, 2000). Conversely, some authors identified the presence of the NADW beyond the Davie Ridge with circulation along its eastern side after a topographic blockage at 14°S (van Aken et al., 2004; Collins et al., 2016). At a depth of more than 4000 mbsl, the Antarctic Bottom Water (AABW) flows from east of the Mozambique ridge to south of the Mozambique Basin. It is then diverted, before heading south along the Madagascar Ridge (Kolla et al., 1980, Fig. 1B). Finally, north of the Mozambique Channel, the North Indian Deep Water (NIDW) flows at a depth of more than 2000 mbsl (Collins et al., 2016; Fig. 1C). It is transported from the Indian Ocean and is present in the northern part of the channel, near the Glorieuses Islands (DiMarco et al., 2002; Fig. 1B). Very few studies have examined the NIDW flow path after its arrival in northern Madagascar and its passage through the Glorieuses Islands. However, new hydrographic data, based on conductivity, temperature, pressure, dissolved oxygen and salinity measurements, allowed to identify the AAIW, NADW and NIDW water masses beyond the ridge and have proposed new circulation patterns (DiMarco et al., 2002; van Aken et al., 2004; Collins et al., 2016).

### 2.3. Geochemical approach

Dissolved Nd in seawater mainly originates from aerosols and continental inputs, through rivers (Goldstein et al., 1984; Goldstein and Jacobsen, 1988; Elderfield et al., 1990; Tachikawa et al., 1997; Ingri et al., 2000; Bayon et al., 2015; van der Lubbe et al., 2016). The Nd isotope composition in seawater can be modified by particulate and dissolved exchange processes along continental margins termed “boundary exchange” (Lacan and Jeandel, 2001, 2005; Rempfer et al., 2011; Pearce et al., 2013. Wilson et al., 2012). In addition, submarine groundwater discharge and benthic fluids from the pore waters of the sediments have been identified as significant sources for Nd in the contributing to REE fluxes to the oceans (Johannesson et al., 2011; Abbott et al., 2015a, 2015b; Haley et al., 2017). However, the relative contribution of these inputs to the overall Nd balance in seawater is still described according to geographic areas (Jones et al., 1994). Ocean Nd

residence time is also still debated and supposedly ranges between 600 and 2000 years (Jeandel et al., 1995; Tachikawa et al., 2003; Arsouze et al., 2009; Rempfer et al., 2011), whereas the mixing time of the deep ocean is about 1500 years (Broecker et al., 1982). While being aware of significant changes in local Nd isotope exchange processes or sources, the Nd isotope composition of intermediate and deep waters is therefore expected to be controlled predominantly by conservative mixing between water masses (Goldstein and Hemming, 2003). Nd isotopes are therefore considered as a quasi-conservative tracer of water mass chemistry with potentially great interest in paleoceanographic studies (Frank, 2002; Goldstein and Hemming, 2003). Previous studies of Fe-Mn crusts, nodules and seawater demonstrated that the Atlantic, Indian and Pacific basins each have a distinct and characteristic range in Nd isotope compositions (O'Nions et al., 1978; Piepgras et al., 1979). Consequently, Nd isotopes can be used to trace water sourcing and mixing in both the present and past oceans (Piepgras and Wasserburg, 1980, 1982, 1987; Piepgras and Jacobsen, 1988; Jeandel et al., 2013; Amakawa et al., 2019).

The variations of Nd isotope compositions are expressed as:

$$\varepsilon_{Nd} = \left( \frac{^{143}Nd/^{144}Nd\ (meas.)}{^{143}Nd/^{144}Nd\ (CHUR)} - 1 \right) \times 10^4 \quad (1)$$

where the CHUR (Chondritic Uniform Reservoir) value is 0.512638 (Jacobsen and Wasserburg, 1980). Nd isotope compositions can show significant variations related to erosion and dissolution of rocks in the source regions of water masses. The $\varepsilon_{Nd}$ values of the Pacific Ocean range between 0 and −6 resulting from the erosion of very young volcanic rocks derived from the earth mantle mixed with continental inputs that are unradiogenic (Piepgras and Jacobsen, 1988; Shimizu et al., 1994). The water masses of the North Atlantic have $\varepsilon_{Nd}$ values between −12 and −14 resulting from erosion of old Canadian shield continental rocks while those of the South Atlantic have $\varepsilon_{Nd}$ values between −9 and −11, linked to the mixture between the unradiogenic values of the North Atlantic and the more radiogenic values of the Pacific (Piepgras et al., 1979; Piepgras and Wasserburg, 1982, 1987; Jeandel, 1993). Finally, the Nd isotope composition in the Indian Ocean is a result of the mixture of unradiogenic values of the Atlantic and more radiogenic values of the Pacific Ocean. Its composition ranges between $\varepsilon_{Nd} = -7$ and −8.5 (Bertram and Elderfield, 1993; Arsouze et al., 2007; Wilson et al., 2012). Using Nd isotopes as a tracer of ocean water masses in each ocean basin, it is possible to estimate the respective Atlantic and Pacific contributions to the Indian Ocean by a mixing between the Northwest Atlantic and the Southern Ocean. The equation for conservative Nd isotopic mixing M of the NADW and the Circumpolar Deep Water (CDW) is given by:

$$\varepsilon_{Nd\ (M)} = \frac{X_{(NADW)}\ C_{(NADW)}\ \varepsilon_{Nd\ (NADW)} + \left(1 - X_{(NADW)}\right)\ C_{(CDW)} \varepsilon_{Nd\ (CDW)}}{X_{(NADW)}\ C_{(NADW)} + \left(1 - X_{(NADW)}\right)\ C_{(CDW)}} \quad (2)$$

where $\varepsilon_{Nd}$ and C are described as the Nd isotope composition and concentration respectively and, X as the mixing proportion. The calculation is based on a Nd isotope composition of $\varepsilon_{Nd} = -13$ and a concentration of 25 pmol/kg for the NADW (Piepgras and Wasserburg, 1982, 1987; Jeandel, 1993) and, a Nd isotope composition between $\varepsilon_{Nd} = -4$ and −6 and a concentration of 20 pmol/kg for the CDW (Piepgras and Wasserburg, 1982; Piepgras and Jacobsen, 1988; Jeandel et al., 2013). Thus, for a Nd isotope composition of $\varepsilon_{Nd} = -7$, the Indian water masses can be composed of 15% to 30% of Atlantic water masses and 70% to 85% of Pacific water masses with Atlantic $\varepsilon_{Nd} = -13$ and Pacific between $\varepsilon_{Nd} = -4$ and −6, while for a Nd isotope composition of $\varepsilon_{Nd} = -8.5$, the Indian water masses can be composed of 25% to 45% of Atlantic water masses and 55% to 75% of Pacific water masses with the same Atlantic and Pacific $\varepsilon_{Nd}$. These calculations are consistent with the method used by Frank et al. (2002) whereby a linear mixing relation between the two Nd end-member water masses is assumed because the Nd concentrations in the NADW and CDW do not present a systematic difference. We applied this approach to calculate NADW contributions to the Mozambique Channel. Table 1 presents a summary of Nd isotope compositions of the main water masses in the Mozambique Channel.

## 3. Material and methods

### 3.1. Fe-Mn crust sampling

This work is based on 29 Fe-Mn crust samplings. Locations, depths and other details are given in Table 2 for each sample. 27 were recovered in the Mozambique Channel during the PAMELA-MOZ1 cruise onboard the RV *L'Atalante* (Olu, 2014), as part of the PAMELA (Passive Margin Exploration Laboratory) research project. During this expedition, 22 dredging operations were carried and a total of 186 samples were recovered, including 74 Fe-Mn crusts. 2 other Fe-Mn crusts were recovered during the NOSICAA-MD06 cruise (Agulhas Plateau, sample MNHN-GS-DR75–0012; Leclaire, 1975) and the RIDA-MD39 expedition (western slope of the Davie Ridge, Paisley Mount, sample MNHN-GS-DR84–0026; Leclaire, 1984), conducted by the National Museum of Natural History (MNHN).

Finally, this study is based on 14 sampling stations distributed from the Agulhas Plateau in the south to the Glorieuses Islands north of the Davie Ridge at depths ranging from 580 and 2650 mbsl (Fig. 1A, Table 2), allowing to focus on the geochemical records of all water masses (surface, intermediate and deep).

### 3.2. Nd isotope measurements

After macroscopic examination, approximately 100 mg of sample were collected from scraping the surface layer of the Fe-Mn crusts. The sampling corresponds to the first 100 μm of the sample, i.e. the last elementary adsorption on Fe and Mn oxyhydroxides, and thus the modern state of water mass geochemistry (Albarède and Goldstein, 1992; Albarède et al., 1997), in the order of 20 to 80 ka due to the slow accretion rates of the studied samples ranging from 1.3 to 5.2 mm/Ma, with an average growth rate of 3.1 mm/Ma in all the samples (Bourlès et al. unpublished data). The powders were first dissolved in closed screw-top Teflon vials (Savillex) at about 100 °C for one day using 3 ml of 6 M HCl. The vials where then opened for evaporation at about 130 °C. After evaporation to dryness, approximately 2 ml of aqua regia (10 M HCl + 14 M $HNO_3$) was added, and the vials were capped and put back on the hot plate overnight at about 100 °C. The samples were then dried again and taken up in about 6 ml of Quartex 6 M HCl ("mother solutions"). For of Nd isotope compositions analysis, a 2 ml aliquot of the mother solution was dried, and the residue was taken up in about 0.5 ml of Quartex 14.4 M $HNO_3$ for one hour at 90 °C. The vials where then opened for evaporation at about 90 °C. After evaporation, 1 ml of 1 M

**Table 1**
Water masses abbreviations used in this study together with their corresponding depth range and $\varepsilon_{Nd}$ signatures.

| Abbreviations | Water masses | Depth range (mbsl) | εNd |
|---|---|---|---|
| SICW | South Indian Central Water | 200–700 | −8.5 to −7[a] |
| RSW | Red Sea Water | 800–1400 | −8.5 to −7[a] |
| AAIW | Antarctic Intermediate Water | 800–1500 | −9 to −8[b] |
| NIDW | North Indian Deep Water | 2000–3000 | −8.5 to −7[a] |
| NADW | North Atlantic Deep Water | 1500–3500 | −13 to −9[c] |

[a] Bertram and Elderfield (1993), Arsouze et al. (2007).
[b] Piepgras and Wasserburg (1982), Jeandel (1993), Arsouze et al. (2007), Amakawa et al. (2013).
[c] Piepgras and Wasserburg (1987), Jeandel (1993), Rickli et al. (2009), Tachikawa et al. (2017).

**Table 2**
International Geo Sample Number (IGSN), location, depth and $\varepsilon_{Nd}$ values of the studied Fe-Mn crusts from the PAMELA-MOZ1 (Olu, 2014), NOSICAA-MD06 (Leclaire, 1975) and RIDA-MD39 (Leclaire, 1984) oceanographic expeditions.

| Cruise | Dredge | Sample | IGSN | Location | Latitude | Longitude | Depth range (mbsl) | $^{143}Nd/^{144}Nd$ | 2σ ($10^{-6}$) | εNd | Percent NADW[b] |
|---|---|---|---|---|---|---|---|---|---|---|---|
| PAMELA-MOZ1 | DR01 | MOZ1-DR01–01 | BFBG-155073 | Glorieuses Islands | 11°47′S | 47°54′E | 2400–2650 | 0.512255 | 4 | −7.5 | 21–39 |
| | DR04 | MOZ1-DR04–01 | BFBG-155082 | Glorieuses Islands | 11°28′S | 47°32′E | 1780–2000 | 0.512225 | 8 | −8.1 | 29–45 |
| | DR04 | MOZ1-DR04–03 | BFBG-155084 | Glorieuses Islands | 11°28′S | 47°32′E | 1780–2000 | 0.512227 | 8 | −8.0 | 29–45 |
| | DR04 | MOZ1-DR04–04 | BFBG-155085 | Glorieuses Islands | 11°28′S | 47°32′E | 1780–2000 | 0.512218 | 6 | −8.2 | 31–47 |
| | DR04 | MOZ1-DR04–23 | BFBG-169883 | Glorieuses Islands | 11°28′S | 47°32′E | 1780–2000 | 0.512208 | 4 | −8.4 | 34–49 |
| | DR10 | MOZ1-DR10–04 | BFBG-155152 | Macua Mount | 16°12′S | 41°38′E | 1000–1400 | 0.512226 | 4 | −8.0 | 29–45 |
| | DR10 | MOZ1-DR10–05 | BFBG-155153 | Macua Mount | 16°12′S | 41°38′E | 1000–1400 | 0.512237 | 6 | −7.8 | 26–42 |
| | DR11 | MOZ1-DR11–01 | BFBG-155160 | Jeffrey Ridge | 16°10′S | 42°30′E | 2400–2450 | 0.512180 | 4 | −8.9 | 42–55 |
| | DR11 | MOZ1-DR11–03 | BFBG-155162 | Jeffrey Ridge | 16°10′S | 42°30′E | 2400–2450 | 0.512191 | 4 | −8.7 | 39–52 |
| | DR11 | MOZ1-DR11–05 | BFBG-155164 | Jeffrey Ridge | 16°10′S | 42°30′E | 2400–2450 | 0.512197 | 4 | −8.6 | 37–51 |
| | DR11 | MOZ1-DR11–07 | BFBG-155166 | Jeffrey Ridge | 16°10′S | 42°30′E | 2400–2450 | 0.512157 | 8 | −9.4 | 48–60 |
| | DR12 | MOZ1-DR12–09 | BFBG-155179 | Juan de Nova | 17°1′S | 42°36′E | 1350–1650 | 0.512231 | 8 | −7.9 | 28–44 |
| | DR12 | MOZ1-DR12–14 | BFBG-155184 | Juan de Nova | 17°1′S | 42°36′E | 1350–1650 | 0.512245 | 6 | −7.7 | 24–41 |
| | DR12 | MOZ1-DR12-V | BFBG-169884 | Juan de Nova | 17°1′S | 42°36′E | 1350–1650 | 0.512232 | 4 | −7.9 | 27–44 |
| | DR13 | MOZ1-DR13–07 | BFBG-155191 | North Sakalaves Mounts | 17°59′S | 41°39′E | 1300–1600 | 0.512202 | 6 | −8.5 | 36–50 |
| | DR14 | MOZ1-DR14–04 | BFBG-155201 | Sakalaves Mounts | 18°39′S | 41°51′E | 580–650 | 0.512249 | 4 | −7.6 | 23–40 |
| | DR15 | MOZ1-DR15–10 | BFBG-155211 | South Sakalaves Mounts | 18°57′S | 41°45′E | 1200–1250 | 0.512236 | 4 | −7.8 | 26–43 |
| | DR15 | MOZ1-DR15–14 | BFBG-155215 | South Sakalaves Mounts | 18°57′S | 41°45′E | 1200–1250 | 0.512247 | 8 | −7.6 | 23–40 |
| | DR16 | MOZ1-DR16–05 | BFBG-155220 | Bassas da India | 21°36′S | 39°38′E | 1350–1600 | 0.512195 | 4 | −8.6 | 38–51 |
| | DR16 | MOZ1-DR16–06 | BFBG-155221 | Bassas da India | 21°36′S | 39°38′E | 1350–1600 | 0.512172 | 4 | −9.1 | 44–57 |
| | DR17 | MOZ1-DR17–01 | BFBG-155224 | Hall Bank | 21°50′S | 39°10′E | 1700–1900 | 0.512158 | 6 | −9.4 | 48–60 |
| | DR17 | MOZ1-DR17–04 | BFBG-155227 | Hall Bank | 21°50′S | 39°10′E | 1700–1900 | 0.512175 | 6 | −9.0 | 43–56 |
| | DR19 | MOZ1-DR19–01 | BFBG-155233 | Jaguar Bank | 21°44′S | 39°32′E | 1000–1350 | 0.512257 | 24 | −7.4 | 20–38 |
| | DR22 | MOZ1-DR22–01 | BFBG-155243 | Europa | 21°18′S | 40°23′E | 1400–1550 | 0.512216 | 4 | −8.2 | 32–47 |
| | DR22 | MOZ1-DR22–02 | BFBG-155244 | Europa | 21°18′S | 40°23′E | 1400–1550 | 0.512194 | 6 | −8.7 | 38–52 |
| | DR22 | MOZ1-DR22–03 | BFBG-155245 | Europa | 21°18′S | 40°23′E | 1400–1550 | 0.512240 | 8 | −7.8 | 25–42 |
| | DR22 | MOZ1-DR22–06 | BFBG-155248 | Europa | 21°18′S | 40°23′E | 1400–1550 | 0.512221 | 4 | −8.1 | 30–46 |
| RIDA-MD39 | DR84–0026 | DR84–0026 | MNHN-GS-DR84–0026 | Paisley Mount | 14°08′S | 41°29′E | 800–810 | 0.512272 | 4 | −7.1 | 16–35 |
| | DR84–0026 | DR84–02 | | Paisley Mount | 14°08′S | 41°29′E | 800–810 | 0.512272 | 24 | −7.4 [a] | 20–38 |
| | DR84–0033 | DR84–09 | | Macua Mount | 16°12′S | 41°39′E | 700–953 | 0.512274 | 20 | −7.1 [a] | 16–35 |
| NOSICAA-MD06 | DR75–0012 | DR75–0012 | MNHN-GS-DR75–0012 | Agulhas Plateau | 37°32′S | 27°00′E | 2550–2550 | 0.512119 | 6 | −10.1 | 60–68 |
| | DR75–0012 | DR75–08 | | Agulhas Plateau | 37°32′S | 27°00′E | 2550–2550 | 0.512094 | 26 | −10.6 [a] | 66–73 |

[a] Albarède et al. (1997).
[b] Numbers are percentages of NADW calculated with Pacific water mass end-member values of $\varepsilon_{Nd} = -4$ and $-6$ (Frank et al., 2002).

$HNO_3$ was added and the samples were centrifuged. The REE fraction was separated using Eichrom® Tru spec Resin and the Nd separation was carried out using Eichrom® Ln spec Resin on volumetrically calibrated Teflon columns following an analytical procedure modified from Pin et al. (1994). Nd fractions were loaded on double Re filaments and measured in static mode on a multicollector Thermal Ionization Mass Spectrometer (ThermoScientific Triton) at the "Pôle de Spectrométrie Océan" in Brest, France. The measured $^{143}Nd/^{144}Nd$ ratio was corrected for mass fractionation by normalizing to $^{146}Nd/^{144}Nd = 0.7219$ and the $\varepsilon_{Nd}$ values were calculated as expressed in Eq. (1). Nd isotope composition of standard JNdi was analyzed to monitor instrumental drift. The averaged result of $^{143}Nd/^{144}Nd = 0.512088 \pm 7$ ($2\sigma \times 10^{-6}$; $n = 14$) was consistent with its certified value of $^{143}Nd/^{144}Nd = 0.512115 \pm 7$ ($2\sigma \times 10^{-6}$; Tanaka et al., 2000) corresponding to a LaJolla Nd isotope composition value of $^{143}Nd/^{144}Nd = 0.511858 \pm 7$ ($2\sigma \times 10^{-6}$; Lugmair et al., 1983), so that no instrumental bias had to be taken in account. The standard deviation of this average is ±0.13 $\varepsilon_{Nd}$ unit and associated to each sample analysis. Blank values are below an average of 100 pg and therefore negligible in all cases.

## 4. Nd isotope compositions

The Nd isotope signatures from the surface layer of the Fe-Mn crusts highlight the large variability (between $\varepsilon_{Nd} = -7.1$ and $-10.1$) of water mass compositions (Table 2, Fig. 2). In several hydrodynamic and geochemical studies (Toole and Warren, 1993; Jeandel et al., 1995; McCave et al., 2005; Ullgren et al., 2012; Collins et al., 2016), an average water depth of 1500 mbsl is considered to separate intermediate layers (AAIW between 800 and 1500 mbsl, RSW between 900 and 1200 mbsl) from deep layers (NADW and NIDW at more than 1500–2000 mbsl). Therefore, Nd isotope composition of samples located above and below 1500 mbsl will be presented separately (Fig. 3). However, one must note that 4 dredge operations (including 9 samples) were performed both above and just below 1500 mbsl (Fig. 2). For convenience, these results will be included with those obtained on Fe-Mn crusts located strictly above 1500 mbsl; but will be discussed separately.

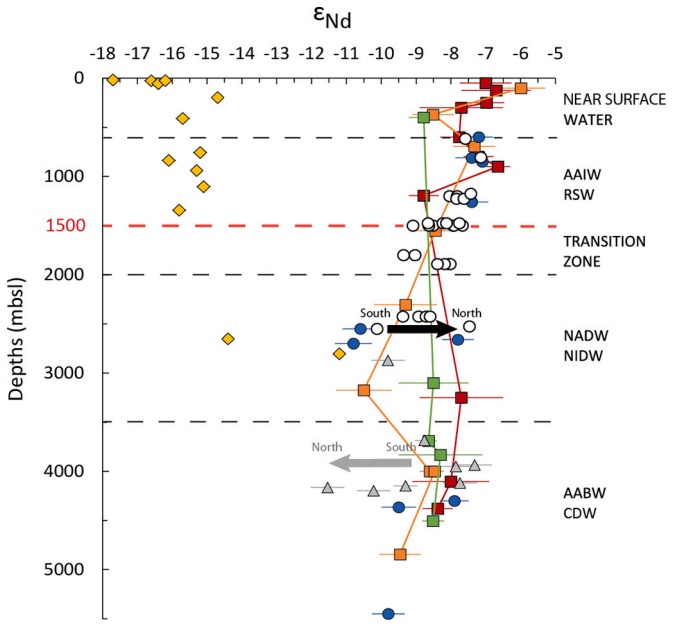


**Fig. 2.** Plot comparing $\varepsilon_{Nd}$ data obtained from surface layer of Fe-Mn crusts (this study; white points) to $\varepsilon_{Nd}$ values from the region. The yellow diamonds represent $\varepsilon_{Nd}$ data from Zambezi sediments along the Mozambique Margin (van der Lubbe et al., 2016); the grey triangles show $\varepsilon_{Nd}$ values from uncleaned foraminiferal coatings from the Madagascar Basin and Mascarene Basin (Wilson et al., 2012) and the blue points correspond to $\varepsilon_{Nd}$ data from Fe-Mn nodules (Albarède et al., 1997). Seawater $\varepsilon_{Nd}$ profiles are represented in green, orange and red respectively from the Madagascar Basin (CD1504/CD1505), the Somali Basin (CD1506/CD1507) and the Mascarene Basin (CD1502/CD1503; Bertram and Elderfield, 1993). Error bars on the data points represent 2σ. The grey arrow represents the Nd isotope variation of Wilson et al. (2012) study linked to unradiogenic Nd inputs along the Madagascan margin, whereas the black arrow corresponds to the trend of our study showing the opposite of that expected with a boundary exchange along an unradiogenic shelf. Black dotted lines and labels show the western Indian Ocean water column structure. Red dotted line corresponds to the average water depth of 1500 mbsl considered to separate intermediate and deep layers.(For interpretation of the references to color in this figure legend, the reader is referred to the web version of this article.)

17 Fe-Mn crusts located above 1500 mbsl were analyzed in this study. South of the Davie Ridge, dredge 19 (DR19) is the shallowest (1000–1350 mbsl). This operation was carried out north of the Jaguar Bank and presents a sample crust with a Nd isotope composition of $\varepsilon_{Nd} = -7.4$ (Table 2, Fig. 3A). The southernmost samples, from dredge 22 (DR22; 1400–1570 mbsl), are located near Europa. For these samples, $\varepsilon_{Nd}$ range from −7.8 to −8.7 ($n = 4$). North of these 2 dredges, near Bassas da India, samples collected with dredge 16 (DR16; 1350–1600 mbsl) show unradiogenic compositions of $\varepsilon_{Nd} = -8.6$ and −9.1. In the southern part of the Davie Ridge, south of the Sakalaves Mounts (DR15; 1200–1250 mbsl), the compositions are more radiogenic with $\varepsilon_{Nd}$ values of −7.8 and −7.6. At the summit of the Sakalaves Mounts (DR14; 580–650 mbsl), the crust presents an $\varepsilon_{Nd} = -7.6$, whereas north of the Sakalaves Mounts (DR13; 1000–1400 mbsl), the composition is less radiogenic with a value of $\varepsilon_{Nd} = -8.5$. In the northern part of the Davie Ridge, we analyzed 2 Nd isotope compositions on 2 different crusts. The Fe-Mn crust located on the Macua Mount (DR10; 1000–1400 mbsl) shows radiogenic compositions of $\varepsilon_{Nd} = -7.8$ and −8.0, whereas the sample located on the Paisley Mount on the western slope of the Davie Ridge (DR84–0026; 810 mbsl) exhibits an isotopic composition of $\varepsilon_{Nd} = -7.1$. The analyzed samples from the southwest of Juan de Nova (DR12; 1350–1650 mbsl) show $\varepsilon_{Nd}$ values ranging from −7.7 to −7.9 ($n = 3$).

Below 1500 mbsl, 12 Fe-Mn crusts provided Nd isotope compositions. The deepest crust was recovered on the Agulhas Plateau (DR75–0012; 2550 mbsl), 2500 km south of the Davie Ridge (Fig. 1A). It provides an $\varepsilon_{Nd}$ value of −10.1 (Table 2, Fig. 3B). Further north, on the east of the Hall Bank (DR17; 1700–1900 mbsl), the $\varepsilon_{Nd}$ are −9.0 and −9.4. North of the Davie Ridge, the analyzed samples from the Jeffrey Ridge (DR11; 2400–2450 mbsl) show values ranging between $\varepsilon_{Nd} = -8.6$ and −9.4 ($n = 4$), and the results from the samples located at the Glorieuses Islands (DR01; 2400–2650 mbsl, DR04; 1750–2050 mbsl) attest to more radiogenic Nd isotope compositions in the range of $\varepsilon_{Nd} = -7.5$ to −8.4 ($n = 5$).

## 5. Discussion

### 5.1. Characterization of the $\varepsilon_{Nd}$ records

#### 5.1.1. Impact of glacial/interglacial variability

Given the relatively slow accretion rates, the 29 studied samples span a time range between 20 and 80 ka, including the record variations of marine isotope stages (MIS) 1 (present to 14 ka), MIS 2 (14 to 29 ka), MIS 3 (29 to 57 ka), MIS 4 (57 to 71 ka) and to a lesser extent MIS 5 (71 to 130 ka). Changes in the broad patterns of ocean circulation and particles fluxes have been identified between the interglacial MIS 1, 3, 5 and the glacial stages 2, 4 (Curry and Lohmann, 1982; Boyle, 1988; Broecker and Denton, 1990; Rutberg et al., 2000; Bayon et al., 2002; Yu et al., 2008; Roberts et al., 2010; Piotrowski et al., 2004, 2005, 2012; Wei et al., 2016). In particular, Nd isotope variations of Fe-Mn oxide coatings and bulk sediment reductive leachates from southeast Atlantic cores, located near the Cape Basin, indicate cyclic changes with climate stages (Rutberg et al., 2000; Piotrowski et al., 2004, 2005, 2012): during the last glacial maximum (LGM, MIS 2) and the MIS 4 the cores recorded radiogenic $\varepsilon_{Nd}$ values ($-6 > \varepsilon_{Nd} > -7$), while the Nd isotope signatures were unradiogenic ($-9 > \varepsilon_{Nd} > -10$) during the interglacial timescales

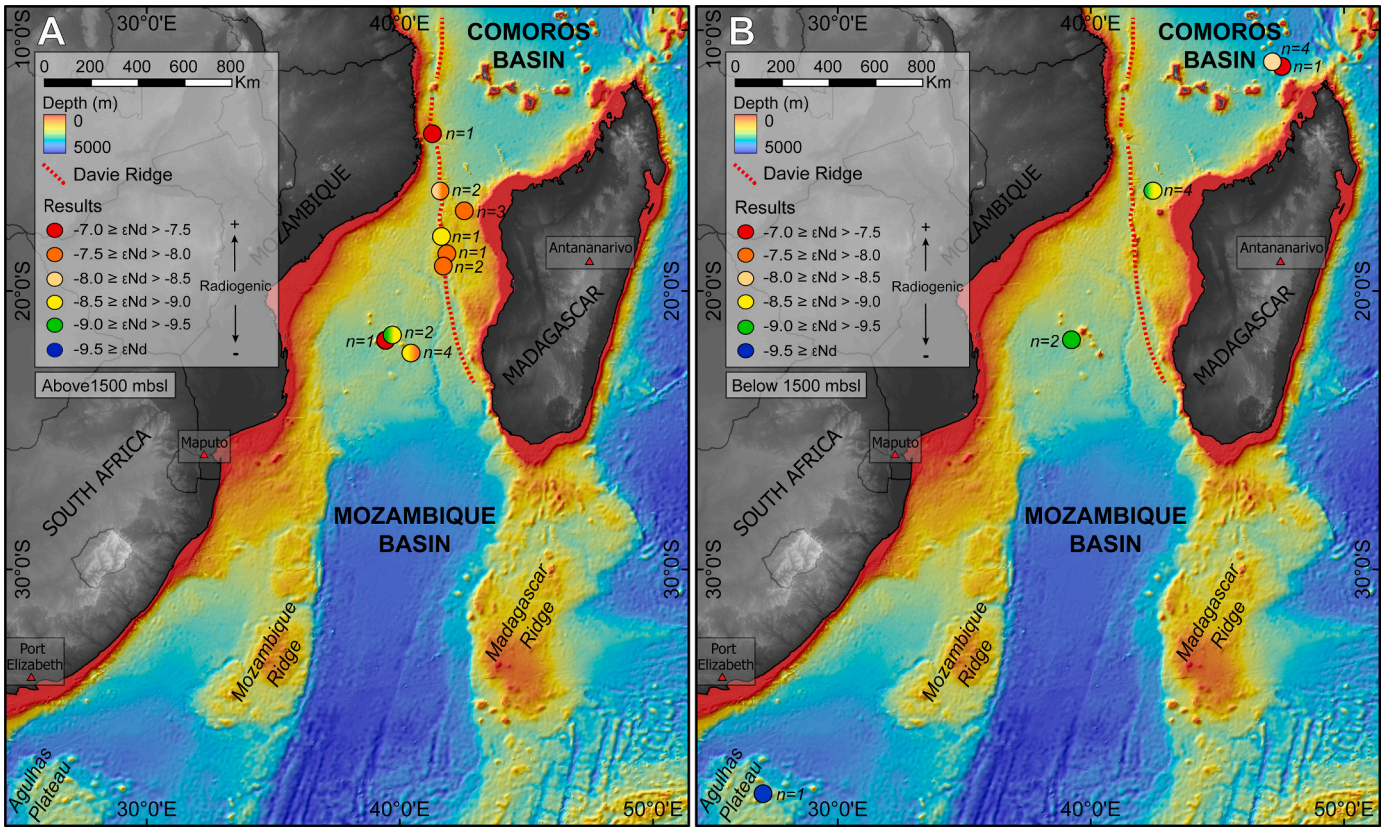


**Fig. 3.** (A) Bathymetry of the Mozambique Channel (data from GEBCO and PAMELA cruises) with $\varepsilon_{Nd}$ values of the samples located above 1500 mbsl. (B) Bathymetry of the Mozambique Channel (data from GEBCO and PAMELA cruises) showing $\varepsilon_{Nd}$ values of the samples located below 1500 mbsl. "*n*" represents the number of samples analysed per dredge.

(MIS 1, 3, 5). This variation characterized by a shift of 2 to 3 $\varepsilon_{Nd}$ units suggests less NADW flux reached the Southern Ocean during cold stages but an increasing export of NADW during the warm climate intervals (Rutberg et al., 2000), with direct influence on the Nd isotope signature of the Indian deep waters during the MIS (Piotrowski et al., 2009).

However, it has been demonstrated in several studies that, given their slow accumulation rates of few mm/Ma, the Nd isotope records from the outer layers of Fe-Mn oxides represent averages of several glacial/interglacial cycles (Abouchami et al., 1997; Albarède and Goldstein, 1992). The short-term changes in the patterns of ocean circulation and particle fluxes have had only minor integrated effects (Abouchami et al., 1997; Albarède and Goldstein, 1992). Insofar as the $\varepsilon_{Nd}$ measurements of this work are going to be contrasted to present-day seawater Nd isotope signatures, it is important to notice that their analysis provides time-integrated information on the $\varepsilon_{Nd}$ variations, which can be compared with the modern oceanic circulation (Albarède et al., 1997; Piotrowski et al., 2009; Wilson et al., 2012).

### 5.1.2. *Influence of unradiogenic African margin on $\varepsilon_{Nd}$ signatures*

As explained in § 2.1, the African continental margin is characterized by an unradiogenic signature of $\varepsilon_{Nd} \sim -20$ (Jeandel et al., 2007), which represents an average of South African Archean cratonic rocks (Jelsma et al., 1996; Möller et al., 1998; De Waele et al., 2006; Grantham et al., 2011) and younger volcanic sources (Grousset et al., 1992; Jourdan et al., 2007; Fig. 1B). Studies in the modern ocean have suggested that inputs of river loads (van der Lubbe et al., 2016; Rahlf et al., 2020) as well as exchange between particulate and dissolved fractions along African continental margins (Rickli et al., 2010; Stichel et al., 2012b; Wilson et al., 2012) may have an important impact on the Nd isotope composition of Atlantic and Indian Oceans. In addition, recent studies have demonstrated that the pore waters can strongly control the REE compositions of the bottom waters (Haley and Klinkhammer, 2003; Schacht et al., 2010; Abbott et al., 2015a, 2015b; Du et al., 2016; Haley et al., 2017; Abbott, 2019).

In the Mozambique Channel, surface waters of the Zambezi and Limpopo discharge have unradiogenic signatures ($-14.7 > \varepsilon_{Nd} > -15.5$ and up to $-22.4$ respectively; Rahlf et al., 2020). This is thought to influence highly unradiogenic Nd isotope signatures ($\varepsilon_{Nd} = -18.9$ and $\varepsilon_{Nd} = -17.6$) of surface waters (<600 mbsl) linked to the AC inflow (Stichel et al., 2012b; Rahlf et al., 2020). Moreover, it has been observed that Nd isotope compositions of water masses can be modified up to a spatial variability of ~4 $\varepsilon_{Nd}$ units due to the boundary exchange process between seawater and the unradiogenic Madagascan shelf ($\varepsilon_{Nd} \sim -25$; Paquette et al., 1994; Kröner et al., 2000), as shown by Wilson et al. (2012). Our work presents 1 sample from near surface water masses (DR14; 580–650 mbsl) and 6 other Fe-Mn crusts from intermediate waters between 800 and 1400 mbsl (DR10, DR15, DR19 and DR84–0026; Fig. 2). These dredges are spatially spread out over 900 km from the Paisley Mount (DR84–0026) to the Jaguar Bank (DR19) and under the influence of the MC, which spreads from the northern part of the Mozambique Channel and is dragged southbound. 6 of them are located north of the Zambezi (DR84–0026, DR10, DR12, DR13, DR14 and DR15) while the other 3 are situated south of the river mouth (DR16, DR19 and DR22; Fig. 1A).

Considering the hypothesis of the Zambezi River loads, the compositions of the samples located in the northern part of the channel are expected to reflect the radiogenic influence of the RSW. Conversely, the crusts located south of the river mouth should indicate unradiogenic Nd isotope signature resulting from continental Nd inputs (Stichel et al., 2012b; Rahlf et al., 2020). In the case of gradual southwards boundary exchange and/or impact of pore waters, it would involve a progressive change of $\varepsilon_{Nd}$ signatures. If the MC acquires unradiogenic composition

during its spreading along the East African margin as suggested by Wilson et al. (2012), we expect to observe a trend from radiogenic values in the northern part of the channel to unradiogenic signature in the south. However, our results show a narrow range from $\varepsilon_{Nd} = -7.1$ to $-8.0$ (Fig. 2) and display no abrupt or continuous variations in the Nd isotope signature along the N-S profile. Indeed, the southernmost sample (DR19) presents a value of $\varepsilon_{Nd} = -7.4$ (Table 2, Fig. 3A), whereas it expected to have the more unradiogenic $\varepsilon_{Nd}$ whether in the case of river inputs, boundary exchange and/or pore waters influence hypotheses. Moreover, the lowest and the highest $\varepsilon_{Nd}$ signatures are observed from DR84–0026 ($\varepsilon_{Nd} = -7.1$) and DR10 ($\varepsilon_{Nd} = -8.0$) located in the northern part of the Mozambique Channel in an distance of 200 km from each other (Fig. 3A). As consequence, our data do not support a major influence of unradiogenic Nd inputs from the river discharges or the continental shelf.

We present 12 samples from the deep water masses (DR01, DR04, DR11, DR17 and DR75–0012; between 1700 and 2550 mbsl; Fig. 2), spatially spread out over 3500 km from the Glorieuses Islands (DR01) to the Agulhas Plateau (DR75–0012; Fig. 3B). In contrast to the crusts from the overlying water masses, these are under the influence of the NADW inflow starting upstream of the south of Africa before entering the Mozambique Channel through the Natal Valley (Toole and Warren, 1993; Fig. 1B). If the unradiogenic Nd isotope addition processes had an impact on the deep water masses, one would predict that this influence would increase as the NADW flows northward. However, the data are increasingly radiogenic towards the north, from $\varepsilon_{Nd} = -10.2$ above the Agulhas Plateau to $\varepsilon_{Nd} = -7.5$ near the Glorieuses Islands (Fig. 3B). Whereas the results of Wilson et al. (2012) present a decreasing radiogenic trend as the boundary exchange occurs, from $\varepsilon_{Nd} = -8.8$ above the Madagascar Ridge to $\varepsilon_{Nd} = -11.5$ in the northeast of the island (Fig. 2). Considering a simple boundary exchange between the African continental margin ($\varepsilon_{Nd} \sim -20$; Jeandel et al., 2007), the NADW arriving from south of southern Africa ($\varepsilon_{Nd} \sim -11$; Rahlf et al., 2020) and a boundary exchange rate of 28% calculated by Wilson et al. (2012), the Nd isotope composition of the crust from DR75–0012 is supposed to be $\varepsilon_{Nd} = -13.5$. Furthermore, if the interaction with the unradiogenic margin is continuous from the Agulhas Plateau to the Glorieuses Islands, the results would present Nd isotope compositions considerably lower than $\varepsilon_{Nd} = -13.5$ in all the crusts from the deep waters (DR17, DR11, DR04 and DR01). It would be the same observation in the context of unradiogenic Nd inputs from river discharges or pore waters. However, this is not apparent in our results ($\varepsilon_{Nd} = -10.2$ from the Agulhas Plateau and $\varepsilon_{Nd} = -7.1$ at the Glorieuses Islands; Fig. 3B) which are too radiogenic to be explained by the boundary exchange between the NADW and the African shelf.

Finally, the isotopic data of our work are consistent with previous studies (Fig. 2), which are focused on the conservative water mass mixing process in the same geographic area on Fe-Mn crusts (Albarède et al., 1997) and in seawater (Bertram and Elderfield, 1993). Although a slight contribution of the unradiogenic inputs from the African margin cannot be completely ruled out, we assume that our results are mainly due to water mass mixing process. The following sections will therefore discuss the identification of water masses from Nd isotope compositions and their hydrographic frameworks through the Mozambique Channel.

### 5.2. Intermediate layers and Indian water influence (< 1500 mbsl)

Above 1500 mbsl, 1 sample provides information on the superficial water masses. Located on the Sakalaves Mounts and at shallow depths (DR14; 580–650 mbsl), this crust displays a value of $\varepsilon_{Nd} = -7.6$ likely corresponding to the Nd isotope composition of the SICW (Fig. 1C, Table 1). This is the only result on this water mass and thus it will not be discussed further here.

However, the 6 other samples are located between 800 and 1400 mbsl (DR10, DR15, DR19 and DR86–0026), illustrating the Nd isotope composition of intermediate water masses. With an range of values between $\varepsilon_{Nd} = -7.1$ and $-8.0$, these Fe-Mn crusts recorded Indian intermediate water (Tables 1 and 2). This intermediate layer could correspond to the RSW arriving from the north of the Mozambique Channel, following the African continental margin southward (Beal et al., 2000) to the Paisley Mount and the Macua Mount (Fig. 1). The hydrographic flow path of these Indian intermediate water masses south of the Davie Ridge (south of the Sakalaves Mounts and Jaguar Bank) could be explained by the presence of anticyclonic eddies passing through the narrowest part of the Mozambique Channel carrying saline and warm RSW southward as described previously by Ullgren et al. (2012) and Miramontes et al. (2019).

### 5.3. Transition zone between intermediate and deep layers

The 10 samples from the north of the Sakalaves Mounts (DR13), near Juan de Nova (DR12), Bassas da India and Europa (DR16 and DR22) present $\varepsilon_{Nd}$ in the range of $-7.7$ to $-9.1$ (Table 2, Fig. 2). Both extremes are marked by the influence of distinct water masses. The $\varepsilon_{Nd} = -9.1$ (DR16, Bassas da India) is lower and may point out to an Atlantic inflow in the Mozambique Basin. Other values such as $\varepsilon_{Nd} = -8.7$ (DR22, Europa), $-8.6$ (DR16, Bassas da India) and $-8.5$ (DR13, North of the Sakalava Mounts) also suggest a slight influence of Atlantic currents (Table 1). North of the Davie Ridge, more radiogenic values measured on crusts located near Juan de Nova ($\varepsilon_{Nd} > -8.0$; $n = 3$) correspond to the Indian intermediate water mass inflow as described in § 5.2. However, dredge 22 shows heterogeneous isotopic compositions with one sample at $\varepsilon_{Nd} = -8.7$ that likely indicate Atlantic influence, but also 2 samples with $\varepsilon_{Nd} > -8.5$ ($-8.2$ and $-8.1$) and one crust with $\varepsilon_{Nd} > -8.0$ ($-7.7$) suggesting the presence of Indian water mass.

Therefore, it is imperative to understand why both Atlantic and Indian water mass inflows are recorded in the same area (Fig. 3A). Two assumptions can be considered. The first is the confrontation of the AAIW and RSW intermediate currents whose depths and thicknesses are relatively similar (Fig, 1C, Table 1). In this case, the Nd isotope variations observed would be related to mixing of the unradiogenic AAIW that enters from the south of the channel, and the more radiogenic RSW arriving from the northwest part of the Mozambique Channel (Fig. 1C). The unradiogenic results would be related to a strong AAIW influence whereas the more radiogenic values would correspond to a robust RSW inflow in the channel. However, the integrated time in these surface scraping is in the order of 30 to 80 ka due to the slow accretion rates of this studied samples ranging from 1.3 to 3.6 mm/Ma. It provides time-integrated information on the sources of Nd (Albarède et al., 1997; Frank et al., 2002) and, should streamline water mass variations mainly related to glacial and interglacial changes. In this case, the recorded isotopic compositions should be relatively homogeneous. The second hypothesis heeds the depths of the starting and ending points of dredge operations (e.g. DR16; 1600–1350 mbsl), which can lead to the recovery of Fe-Mn crusts that are under the influence of deep water masses (NADW, NIDW) and/or intermediate water masses (RSW, AAIW; Table 1, Fig. 2). Thus, within the same dredge (i.e. DR22; 1400–1550 mbsl), some samples could have recorded the isotopic composition of the intermediate currents while others could have recorded the isotopic signature of a transition zone between intermediate and deep water masses (Fig. 2). In this case, differences in the recorded Nd isotope compositions would be related to the thickness variations of the water masses in the Mozambique Channel over the last 100 ka.

### 5.4. Deep layers (>1500 mbsl)

The Nd isotope compositions, recorded on Fe-Mn crusts located between 1700 and 2650 mbsl, provided a significant number of results ($n = 12$) with a clear isotopic trend from the south to the north of the Mozambique Channel (Fig. 3BB). Southwestern of the Davie Ridge, the crust from the Agulhas Plateau (DR75–0012) presents an unradiogenic result of $\varepsilon_{Nd} = -10.1$ likely reflecting Atlantic deep water arrival in the

Mozambique Channel (Fig. 1B, Table 1). Using the calculation of Frank et al. (2002), the contribution of the NADW is estimated at 60% in the Agulhas Plateau fixing Atlantic seawater $\varepsilon_{Nd} = -13$ and Pacific seawater $\varepsilon_{Nd} = -6$ (68% with Pacific seawater $\varepsilon_{Nd} = -4$; Table 2, Fig. 4). This percentage is supported by the study of Rahlf et al. (2020), which estimates a mixing between a NADW fraction of up to 80–90% with the CDW eastern Cape Basin. The contribution of NADW then decreases southward, reflecting a gradual dilution with southern waters. Its influence is recorded all the way to the Hall Bank with values $\varepsilon_{Nd} = -9.0$ and $-9.4$ (DR17). In this area the NADW inflow is calculated between 43% and 48% (56% and 60% with Pacific seawater $\varepsilon_{Nd} = -4$; Table 2, Fig. 4). By contrast, in the north of the Mozambique Channel, near the Glorieuses Islands (DR01 and DR04), the Nd isotope compositions are more radiogenic ($-7.5 > \varepsilon_{Nd} > -8.4$; $n = 5$) corresponding to the Indian Ocean influence by the arrival of the NIDW in the Comoros Basin (Fig. 1B, Table 1). In the northern part of the channel, the contribution of the NADW is estimated between 21% and 34% (39% and 49% with Pacific seawater $\varepsilon_{Nd} = -4$; Table 2, Fig. 4). These values correspond to the contributions of Atlantic water masses in the mixing with Pacific water masses in the current Indian Ocean. Therefore, the NADW from the south of the Mozambique Channel does not seem to be present in the northern part of the Comoros Basin. However, less radiogenic compositions (up to $\varepsilon_{Nd} = -9.4$; DR11) were recorded north of the Davie Ridge, on a ridge in the Comoros Basin, 90 km north of Juan de Nova and 700 km southwest of the Glorieuses Islands (Table 2, Fig. 3B). These unradiogenic values cannot be explained solely by the presence of the NIDW in the northern part of the Mozambique Channel. The inflow of the NADW is estimated between 37% and 48% (51% and 60% with Pacific seawater $\varepsilon_{Nd} = -4$; Table 2, Fig. 4). These estimates of the Atlantic inflow show that a significant portion of the NADW crosses the Davie Ridge and flows into the northern part of the channel without reaching the Glorieuses Islands.

### 5.5. NADW northern boundary

This study reveals a trend based on Nd isotope compositions of Fe-Mn crusts from unradiogenic values in the south of the Africa, on the Agulhas Plateau, to more radiogenic values in the north of the Mozambique Channel (Table 2, Fig. 3). For the first time it is possible to identify and quantify the NADW influence in the Mozambique Channel to the Comoros Basin through a geochemical study of Fe-Mn crusts (Fig. 4). The only research carried out on Fe-Mn crusts in this area is that

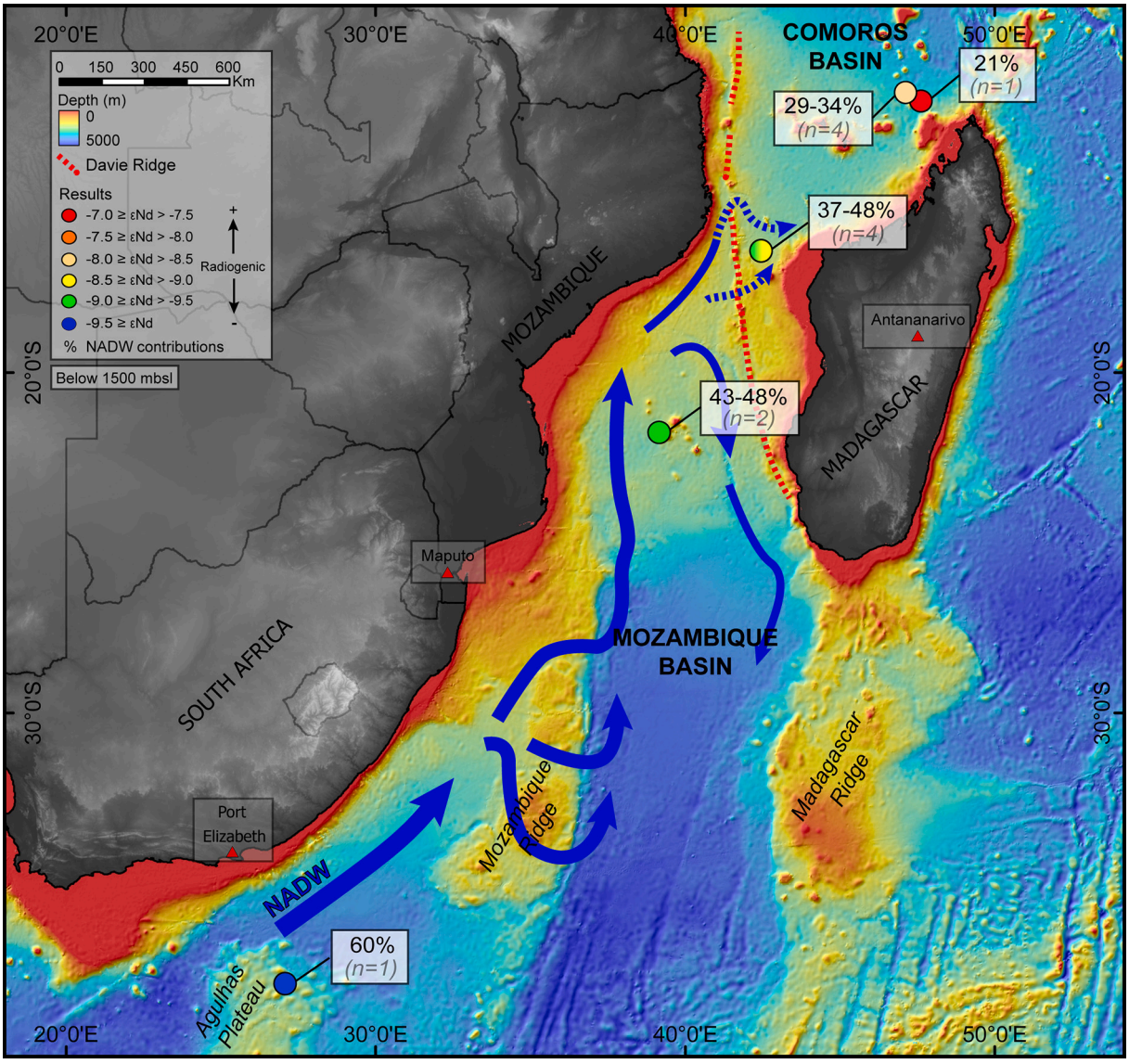


**Fig. 4.** Bathymetry of the Mozambique Channel (data from GEBCO and PAMELA cruises) showing Atlantic waters contributions estimated through the Mozambique Channel (for Pacific $\varepsilon_{Nd} = -6$) and the resulting circulation of NADW. The dashed arrows present a suggestion of potential NADW passages beyond the Davie Ridge.

of Albarède et al. (1997), Fig. 2, indicating unradiogenic value in the southwestern part of the Mozambique Channel as presented before but an isocontour of $\varepsilon_{Nd} = -8$ upstream of the Mozambique Basin and Madagascar. This isotope limit suggests a significant restriction of the NADW input into the Mozambique Channel which is not consistent with our results, suggesting this isotope limit further north and most importantly north of the Davie Ridge (Fig. 4). The differences in the Nd isotope values between both studies are undoubtedly related to the depth of the samples. Indeed, Albarède et al. (1997) were interested in Nd global trends in the oceans. In the centre part of the Mozambique Channel, their isotopic analyses were measured on crusts from surface layers (~600 mbsl; Fig. 2). As described in previous sections, these water masses have Nd isotope signatures from the Indian Ocean (Table 1) and are therefore naturally much more radiogenic than the results of our study, which also focuses on intermediate and deep water mass flow path.

Simultaneously, two major hydrographic studies advance scientific knowledge on the Atlantic and Indian deep currents in the Mozambique Channel. van Aken et al. (2004) noted the influence of the NADW current at depths between 1500 and 2500 mbsl in the channel. This was supported and expanded upon by the hydrographic research of Collins et al. (2016). The NADW and NIDW currents were recorded in the Comoros Basin, according to their salinity and oxygen levels. The current flow path of these deep water masses in the Mozambique Channel is therefore a visible and currently quantified phenomenon. Our study confirms the presence of the NADW in the northern part of the channel and strongly suggests a passage of the NADW beyond the Davie Ridge (Fig. 4), implying that this topographic barrier does not currently act as an impassable obstacle to the circulation of deep currents in the Mozambique Channel.

## 6. Summary and conclusion

Fe-Mn crusts are highly studied ocean resources in terms of their geochemical composition as archives of the chemical composition of water masses. The analysis of 29 crusts sampled in the Mozambique Channel show Nd isotope records ranging from unradiogenic values ($\varepsilon_{Nd} = -10.1$) in the Agulhas Plateau to more radiogenic values ($\varepsilon_{Nd} = -7.5$) north of the Mozambique Channel, near the Glorieuses Islands.

First, this study reveals the presence of the Indian intermediate seawater above 1500 mbsl. Secondly, the crusts dredged at depths between 1300 and 1650 mbsl show significant isotopic variations (between $\varepsilon_{Nd} = -7.7$ and $-9.1$), probably due to their location in a transition zone between intermediate and deep water masses with contrasted Nd isotope signatures. Finally, unradiogenic compositions are recorded beyond the Davie Ridge. These new results suggest significant contributions of the NADW flowing from the south below 1500 mbsl and crossing the Davie Ridge to be recorded in the northern part of the Mozambique Channel, in the Comoros Basin.

This unique collection of crust samples improves our understanding of the Atlantic and Indian water mass flow path in this complex area. As this key area of oceanic mixing has undergone diverse geodynamic movements, it would be interesting to carry out isotope studies on several time series distributed from the Agulhas Plateau to the Glorieuses Islands at different depths (especially in the transition zone). These future studies would allow to identify and understand major geodynamic and oceanographic events in the Mozambique Channel up to the Miocene.

## Declaration of Competing Interest

The authors declare that they have no known competing financial interests or personal relationships that could have appeared to influence the work reported in this paper.

## Acknowledgments

We thank the Captains, crews and onboard scientific teams of the PAMELA-MOZ01 survey onboard the R/V *L'Atalante* and, the RIDA-MD39 and the NOSICAA-MD06 surveys onboard the R/V Marion Dufresne. The oceanographic survey PAMELA-MOZ01, as well as Claire CHARLES PhD are co-funded by TOTAL and IFREMER as part of the PAMELA (Passive Margin Exploration Laboratories) scientific project. The PAMELA project is a scientific project led by Ifremer and TOTAL in collaboration with the Université de Bretagne Occidentale, Université Rennes 1, Université Pierre et Marie Curie, CNRS and IFPEN. The authors are grateful to Anne-Sophie Alix, Philippe Fernagu and Thierry Dalle Mulle for their help and the crust-sample preparation. We also thank the MNHN, Eva Moreno and Lola Johannes for allowing us to access and borrow samples from the RIDA-MD39 and NOSICAA-MD06 oceanographic expeditions belonging to the oceanic collection. We gratefully acknowledge Editor-in-Chief Michele Rebesco, Guest Editor Vittorio Maselli, Jean-Carlos Montero-Serrano and an anonymous reviewer for thorough and thoughtful comments that significantly improved the manuscript.

## References

Abbott, A.N., 2019. A benthic flux from calcareous sediments results in non-conservative neodymium behavior during lateral transport: a study from the Tasman Sea. Geology 47, 363–366. https://doi.org/10.1130/G45904.1.

Abbott, A.N., Haley, B.A., McManus, J., 2015a. Bottoms up: sedimentary control of the deep north Pacific Ocean's εNd signature. Geology 43, 1035. https://doi.org/10.1130/G37114.1.

Abbott, A.N., Haley, B.A., McManus, J., Reimers, C.E., 2015b. The sedimentary flux of dissolved rare earth elements to the ocean. Geochim. Cosmochim. Acta 154, 186–200. https://doi.org/10.1016/j.gca.2015.01.010.

Abouchami, W., Goldstein, S.L., Gazer, S.J.G., Eisenhauer, A., Mangini, A., 1997. Secular changes of lead and neodymium in central Pacific seawater recorded by a Fe-Mn crust. Geochim. Cosmochim. Acta 61, 3957–3974. https://doi.org/10.1016/S0016-7037(97)00218-4.

van Aken, H.M., Ridderinkhof, H., de Ruijter, W.P.M., 2004. North Atlantic deep water in the south-western Indian Ocean. Deep Sea Res. Part Oceanogr. Res. Pap. 51, 755–776. https://doi.org/10.1016/j.dsr.2004.01.008.

Albarède, F., Goldstein, S.L., 1992. World map of Nd isotopes in sea-floor ferromanganese deposits. Geology 20, 761–763. https://doi.org/10.1130/0091-7613(1992)020<0761:WMONII>2.3.CO;2.

Albarède, F., Goldstein, S.L., Dautel, D., 1997. The neodymium isotopic composition of manganese nodules from the Southern and Indian oceans, the global oceanic neodymium budget, and their bearing on deep ocean circulation. Geochim. Cosmochim. Acta 61, 1277–1291. https://doi.org/10.1016/S0016-7037(96)00404-8.

Albarède, F., Simonetti, A., Vervoort, J.D., Blichert-Toft, J., Abouchami, W., 1998. A Hf-Nd isotopic correlation in ferromanganese nodules. Geophys. Res. Lett. 25, 3895–3898. https://doi.org/10.1029/1998GL900008.

Amakawa, H., Tazoe, H., Obata, H., Gamo, T., Sano, Y., Shen, C.-C., 2013. Neodymium isotopic composition and concentration in the Southwest Pacific Ocean. Geochem. J. 47, 409–422. https://doi.org/10.2343/geochemj.2.0260.

Amakawa, H., Yu, T.-L., Tazoe, H., Obata, H., Gamo, T., Sano, Y., Shen, C.-C., Suzuki, K., 2019. Neodymium concentration and isotopic composition distributions in the southwestern Indian Ocean and the Indian sector of the Southern Ocean. Chem. Geol. 511, 190–203. https://doi.org/10.1016/j.chemgeo.2019.01.007.

Aplin, A., Cronan, D., 1985. Ferromanganese oxide deposits from the Central Pacific Ocean, I. Encrustations from the Line Islands Archipelago. Geochim. Cosmochim. Acta 49, 427–436. https://doi.org/10.1016/0016-7037(85)90034-1.

Aplin, A., Michard, A., Albarède, F., 1986. 143Nd/144Nd in Pacific ferromanganese encrustations and nodules. Earth Planet. Sci. Lett. 81, 7–14. https://doi.org/10.1016/0012-821X(86)90096-8.

Arsouze, T., Dutay, J.-C., Lacan, F., Jeandel, C., 2007. Modeling the neodymium isotopic composition with a global ocean circulation model. Chem. Geol. 239, 165–177. https://doi.org/10.1016/j.chemgeo.2006.12.006.

Arsouze, T., Dutay, J.-C., Lacan, F., Jeandel, C., 2009. Reconstructing the Nd oceanic cycle using a coupled dynamical – biogeochemical model. Biogeosciences 6, 2829–2846. https://doi.org/10.5194/bg-6-2829-2009.

Bassias, Y., 1992. Petrological and geochemical investigation of rocks from the Davie fracture zone (Mozambique Channel) and some tectonic implications. J. Afr. Earth Sci. Middle East 15, 321–339. https://doi.org/10.1016/0899-5362(92)90018-8.

Bayon, G., German, C.R., Boella, R.M., Milton, J.A., Taylor, R.N., Nesbitt, R.W., 2002. An improved method for extracting marine sediment fractions and its application to Sr and Nd isotopic analysis. Chem. Geol. 187, 179–199. https://doi.org/10.1016/S0009-2541(01)00416-8.

Bayon, G., Toucanne, S., Skonieczny, C., André, L., Bermell, S., Cheron, S., Dennielou, B., Etoubleau, J., Freslon, N., Gauchery, T., Germain, Y., Jorry, S.J., Ménot, G., Monin, L., Ponzevera, E., Rouget, M.-L., Tachikawa, K., Barrat, J.A., 2015. Rare earth

elements and neodymium isotopes in world river sediments revisited. Geochim. Cosmochim. Acta 170, 17–38. https://doi.org/10.1016/j.gca.2015.08.001.
Beal, L.M., Ffield, A., Gordon, A.L., 2000. Spreading of Red Sea overflow waters in the Indian Ocean. J. Geophys. Res. Oceans 105, 8549–8564. https://doi.org/10.1029/1999JC900306.
Bertram, C.J., Elderfield, H., 1993. The geochemical balance of the rare earth elements and neodymium isotopes in the oceans. Geochim. Cosmochim. Acta 57, 1957–1986. https://doi.org/10.1016/0016-7037(93)90087-D.
Boyle, E.A., 1988. Vertical oceanic nutrient fractionation and glacial/interglacial CO2 cycles. Nature 331, 55–56. https://doi.org/10.1038/331055a0.
Broecker, W.S., Denton, G.H., 1990. The role of ocean-atmosphere reorganizations in glacial cycles. Quat. Sci. Rev. 9, 305–341. https://doi.org/10.1016/0277-3791(90)90026-7.
Broecker, W.S., Peng, T., Beng, Z., 1982. Tracers in the Sea. Lamont-Doherty Geological Observatory, Columbia University.
Christensen, J.N., Halliday, A.N., Godfrey, L.V., Hein, J.R., Rea, D.K., 1997. Climate and Ocean dynamics and the lead isotopic records in pacific ferromanganese crusts. Science 277, 913–918. https://doi.org/10.1126/science.277.5328.913.
Coffin, M.F., Rabinowitz, P.D., 1987. Reconstruction of Madagascar and deep: evidence from the Davie fracture zone and western Somali Basin. J. Geophys. Res. Solid Earth 92, 9385–9406. https://doi.org/10.1029/JB092iB09p09385.
Collins, C., Hermes, J.C., Roman, R.E., Reason, C.J.C., 2016. First dedicated hydrographic survey of the Comoros Basin. J. Geophys. Res. Oceans 121, 1291–1305. https://doi.org/10.1002/2015JC011418.
Curry, W.B., Lohmann, G.P., 1982. Carbon Isotopic changes in benthic foraminifera from the western South Atlantic: reconstruction of glacial abyssal circulation patterns. Quat. Res. 18, 218–235. https://doi.org/10.1016/0033-5894(82)90071-0.
De Waele, B., Liégeois, J.-P., Nemchin, A.A., Tembo, F., 2006. Isotopic and geochemical evidence of proterozoic episodic crustal reworking within the irumide belt of south-central Africa, the southern metacratonic boundary of an Archaean Bangweulu Craton. Precambrian Res. 148, 225–256. https://doi.org/10.1016/j.precamres.2006.05.006.
DiMarco, S.F., Chapman, P., Nowlin, W.D., Hacker, P., Donohue, K., Luther, M., Johnson, G.C., Toole, J., 2002. Volume transport and property distributions of the Mozambique Channel. Deep Sea Res. Part II Top. Stud. Oceanogr. 49, 1481–1511. https://doi.org/10.1016/S0967-0645(01)00159-X.
Du, J., Haley, B.A., Mix, A.C., 2016. Neodymium isotopes in authigenic phases, bottom waters and detrital sediments in the Gulf of Alaska and their implications for paleo-circulation reconstruction. Geochim. Cosmochim. Acta 193, 14–35. https://doi.org/10.1016/j.gca.2016.08.005.
Eisenhauer, A., Gögen, K., Pernicka, E., Mangini, A., 1992. Climatic influences on the growth rates of Mn crusts during the late quaternary. Earth Planet. Sci. Lett. 109, 25–36. https://doi.org/10.1016/0012-821X(92)90071-3.
Elderfield, H., Upstill-Goddard, R., Sholkovitz, E.R., 1990. The rare earth elements in rivers, estuaries, and coastal seas and their significance to the composition of ocean waters. Geochim. Cosmochim. Acta 54, 971–991. https://doi.org/10.1016/0016-7037(90)90432-K.
Fine, R.A., 1993. Circulation of Antarctic intermediate water in the South Indian Ocean. Deep Sea Res. Part Oceanogr. Res. Pap. 40, 2021–2042. https://doi.org/10.1016/0967-0637(93)90043-3.
Flemming, B.W., Kudrass, H.-R., 2018. Large dunes on the outer shelf off the Zambezi Delta, Mozambique: evidence for the existence of a Mozambique Current. Geo-Mar. Lett. 38, 95–106. https://doi.org/10.1007/s00367-017-0515-5.
Frank, M., 2002. Radiogenic isotopes: tracers of past ocean circulation and erosional input. Rev. Geophys. 40, 1. https://doi.org/10.1029/2000RG000094.
Frank, M., O'Nions, R.K., 1998. Sources of Pb for Indian Ocean ferromanganese crusts: a record of Himalayan erosion? Earth planet. Sci. Lett. 158, 121–130. https://doi.org/10.1016/S0012-821X(98)00055-7.
Frank, M., O'Nions, R.K., Hein, J.R., Banakar, V.K., 1999. 60 Myr records of major elements and Pb–Nd isotopes from hydrogenous ferromanganese crusts: reconstruction of seawater paleochemistry. Geochim. Cosmochim. Acta 63, 1689–1708. https://doi.org/10.1016/S0016-7037(99)00079-4.
Frank, M., Whiteley, N., Kasten, S., Hein, J.R., O'Nions, K., 2002. North Atlantic Deep water export to the Southern Ocean over the past 14 Myr: Evidence from Nd and Pb isotopes in ferromanganese crusts. Paleoceanography 17, 12-1–12–9. https://doi.org/10.1029/2000PA000606.
Gaina, C., Torsvik, T.H., van Hinsbergen, D.J.J., Medvedev, S., Werner, S.C., Labails, C., 2013. The African Plate: a history of oceanic crust accretion and subduction since the Jurassic. Tectonophysics 604, 4–25. https://doi.org/10.1016/j.tecto.2013.05.037. Progress in understanding the South Atlantic margins.
Goldstein, S.J., Jacobsen, S.B., 1988. Rare earth elements in river waters. Earth Planet. Sci. Lett. 89, 35–47. https://doi.org/10.1016/0012-821X(88)90031-3.
Goldstein, S.L., Hemming, S.R., 2003. 6.17 - long-lived isotopic tracers in oceanography, paleoceanography, and ice-sheet dynamics. In: Holland, H.D., Turekian, K.K. (Eds.), Treatise on Geochemistry. Pergamon, Oxford, pp. 453–489. https://doi.org/10.1016/B0-08-043751-6/06179-X.
Goldstein, S.L., O'Nions, R.K., Hamilton, P.J., 1984. A Sm-Nd isotopic study of atmospheric dusts and particulates from major river systems. Earth Planet. Sci. Lett. 70, 221–236. https://doi.org/10.1016/0012-821X(84)90007-4.
Gordon, A.L., 1986. Interocean exchange of thermocline water. J. Geophys. Res. Oceans 91, 5037–5046. https://doi.org/10.1029/JC091iC04p05037.
Grantham, G.H., Manhica, A.D.S.T., Armstrong, R.A., Kruger, F.J., Loubser, M., 2011. New SHRIMP, Rb/Sr and Sm/Nd isotope and whole rock chemical data from central Mozambique and western Dronning Maud Land, Antarctica: implications for the nature of the eastern margin of the Kalahari Craton and the amalgamation of Gondwana. J. Afr. Earth Sci. 59, 74–100. https://doi.org/10.1016/j.jafrearsci.2010.08.005.
Grousset, F.E., Biscaye, P.E., Revel, M., Petit, J.-R., Pye, K., Joussaume, S., Jouzel, J., 1992. Antarctic (Dome C) ice-core dust at 18 k.y. B.P.: isotopic constraints on origins. Earth Planet. Sci. Lett. 111, 175–182. https://doi.org/10.1016/0012-821X(92)90177-W.
Haley, B.A., Klinkhammer, G.P., 2003. Complete separation of rare earth elements from small volume seawater samples by automated ion chromatography: method development and application to benthic flux. Mar. Chem. 82, 197–220. https://doi.org/10.1016/S0304-4203(03)00070-7.
Haley, B.A., Du, J., Abbott, A.N., McManus, J., 2017. The impact of benthic processes on rare earth element and neodymium isotope distributions in the oceans. Front. Mar. Sci. 4 https://doi.org/10.3389/fmars.2017.00426.
Halo, I., Backeberg, B., Penven, P., Ansorge, I., Reason, C., Ullgren, J.E., 2014. Eddy properties in the Mozambique Channel: A comparison between observations and two numerical ocean circulation models. Deep Sea Res. Part II Top. Stud. Oceanogr. 100, 38–53. https://doi.org/10.1016/j.dsr2.2013.10.015.
Hein, J.R., Conrad, T.A., Dunham, R.E., 2009. Seamount characteristics and mine-site model applied to exploration- and mining-lease-block selection for cobalt-rich ferromanganese crusts. Mar. Georesour. Geotechnol. 27, 160–176. https://doi.org/10.1080/10641190902852485.
Hein, J.R., Conrad, T.A., Staudigel, H., 2010. Seamount mineral deposits: a source of rare metals for high-technology industries. Oceanography 23, 184–189.
Hein, J.R., Conrad, T.A., Mizell, K., Banakar, V.K., Frey, F.A., Sager, W.W., 2016. Controls on Ferromanganese Crust Composition and Reconnaissance Resource Potential, Ninetyeast Ridge, Indian Ocean.
Heirtzler, J.R., Burroughs, R.H., 1971. Madagascar's paleoposition: new data from the Mozambique Channel. Science 174, 488–490. https://doi.org/10.1126/science.174.4008.488.
Ingri, J., Widerlund, A., Land, M., Gustafsson, Ö., Andersson, P., Öhlander, B., 2000. Temporal variations in the fractionation of the rare earth elements in a boreal river; the role of colloidal particles. Chem. Geol. 166, 23–45. https://doi.org/10.1016/S0009-2541(99)00178-3.
Jacobsen, S.B., Wasserburg, G.J., 1980. Sm-Nd isotopic evolution of chondrites. Earth Planet. Sci. Lett. 50, 139–155. https://doi.org/10.1016/0012-821X(80)90125-9.
Jeandel, C., 1993. Concentration and isotopic composition of Nd in the South Atlantic Ocean. Earth Planet. Sci. Lett. 117, 581–591. https://doi.org/10.1016/0012-821X(93)90104-H.
Jeandel, C., Bishop, J.K., Zindler, A., 1995. Exchange of neodymium and its isotopes between seawater and small and large particles in the Sargasso Sea. Geochim. Cosmochim. Acta 59, 535–547. https://doi.org/10.1016/0016-7037(94)00367-U.
Jeandel, C., Arsouze, T., Lacan, F., Téchiné, P., Dutay, J.-C., 2007. Isotopic Nd compositions and concentrations of the lithogenic inputs into the ocean: a compilation, with an emphasis on the margins. Chem. Geol. 239, 156–164. https://doi.org/10.1016/j.chemgeo.2006.11.013.
Jeandel, C., Delattre, H., Grenier, M., Pradoux, C., Lacan, F., 2013. Rare earth element concentrations and Nd isotopes in the Southeast Pacific Ocean. Geochem. Geophys. Geosyst. 14, 328–341. https://doi.org/10.1029/2012GC004309.
Jelsma, H.A., Vinyu, M.L., Wijbrans, J.R., Verdurmen, E.A.T., Valbracht, P.J., Davies, G. R., Valbracht, P.J., 1996. Constraints on Archaean crustal evolution of the Zimbabwe craton: a U-Pb zircon, Sm-Nd and Pb-Pb whole-rock isotope study. Contrib. Mineral. Petrol. 124, 55–70. https://doi.org/10.1007/s004100050173.
Johannesson, K.H., Chevis, D.A., Burdige, D.J., Cable, J.E., Martin, J.B., Roy, M., 2011. Submarine groundwater discharge is an important net source of light and middle REEs to coastal waters of the Indian River Lagoon, Florida, USA. Geochim. Cosmochim. Acta 75, 825–843. https://doi.org/10.1016/j.gca.2010.11.005.
Jones, C.E., Halliday, A.N., Rea, D.K., Owen, R.M., 1994. Neodymium isotopic variations in North Pacific modern silicate sediment and the insignificance of detrital REE contributions to seawater. Earth Planet. Sci. Lett. 127, 55–66. https://doi.org/10.1016/0012-821X(94)90197-X.
Jourdan, F., Bertrand, H., Schärer, U., Blichert-Toft, J., Féraud, G., Kampunzu, A.B., 2007. Major and trace element and sr, nd, hf, and pb isotope compositions of the karoo large igneous Province, Botswana–Zimbabwe: lithosphere vs mantle plume contribution. J. Petrol. 48, 1043–1077. https://doi.org/10.1093/petrology/egm010.
Kolla, V., Eittreim, S., Sullivan, L., Kostecki, J.A., Burckle, L.H., 1980. Current-controlled, abyssal microtopography and sedimentation in Mozambique Basin, southwest Indian Ocean. Mar. Geol. 34, 171–206. https://doi.org/10.1016/0025-3227(80)90071-7.
Koschinsky, A., Halbach, P., 1995. Sequential leaching of marine ferromanganese precipitates: genetic implications. Geochim. Cosmochim. Acta 59, 5113–5132. https://doi.org/10.1016/0016-7037(95)00358-4.
Koschinsky, A., Stascheit, A., Bau, M., Halbach, P., 1997. Effects of phosphatization on the geochemical and mineralogical composition of marine ferromanganese crusts. Geochim. Cosmochim. Acta 61, 4079–4094. https://doi.org/10.1016/S0016-7037(97)00231-7.
Kröner, A., Hegner, E., Collins, A.S., Windley, B.F., Brewer, T.S., Razakamanana, T., Pidgeon, R.T., 2000. Age and magmatic history of the Antananarivo block, central Madagascar, as derived from zircon geochronology and Nd isotopic systematics. Am. J. Sci. 300, 251–288. https://doi.org/10.2475/ajs.300.4.251.
Kusakabe, M., Ku, T.-L., 1984. Incorporation of Be isotopes and other trace metals into marine ferromanganese deposits. Geochim. Cosmochim. Acta 48, 2187–2193. https://doi.org/10.1016/0016-7037(84)90215-1.
Lacan, F., Jeandel, C., 2001. Tracing Papua New Guinea imprint on the central Equatorial Pacific Ocean using neodymium isotopic compositions and rare earth element patterns. Earth Planet. Sci. Lett. 186, 497–512. https://doi.org/10.1016/S0012-821X(01)00263-1.

Lacan, F., Jeandel, C., 2005. Neodymium isotopes as a new tool for quantifying exchange fluxes at the continent–ocean interface. Earth Planet. Sci. Lett. 232, 245–257. https://doi.org/10.1016/j.epsl.2005.01.004.
Leclaire, L., 1975. NOSICAA-MD06. RV Marion Dufresne. https://doi.org/10.17600/75010711.
Leclaire, L., 1984. RIDA-MD39. RV Marion Dufresne. https://doi.org/10.17600/84010511.
Ling, H.F., Burton, K.W., O'Nions, R.K., Kamber, B.S., von Blanckenburg, F., Gibb, A.J., Hein, J.R., 1997. Evolution of Nd and Pb isotopes in central Pacific seawater from ferromanganese crusts. Earth Planet. Sci. Lett. 146, 1–12. https://doi.org/10.1016/S0012-821X(96)00224-5.
van der Lubbe, H.J.L., Frank, M., Tjallingii, R., Schneider, R.R., 2016. Neodymium isotope constraints on provenance, dispersal, and climate-driven supply of Zambezi sediments along the Mozambique Margin during the past ~45,000 years. Geochem. Geophys. Geosyst. 17, 181–198. https://doi.org/10.1002/2015GC006080.
Lugmair, G.W., Shimamura, T., Lewis, R.S., Anders, E., 1983. Samarium-146 in the early solar system: evidence from neodymium in the allende meteorite. Science 222, 1015–1018. https://doi.org/10.1126/science.222.4627.1015.
Lusty, P.A.J., Hein, J.R., Josso, P., 2018. Formation and occurrence of ferromanganese crusts: earth's storehouse for critical metals. Elements 14, 313–318. https://doi.org/10.2138/gselements.14.5.313.
Lutjeharms, J.R.E., 2006. The Agulhas Current. Springer-Verlag, Berlin Heidelberg.
Mahoney, J., Nicollet, C., Dupuy, C., 1991. Madagascar basalts: tracking oceanic and continental sources. Earth Planet. Sci. Lett. 104, 350–363. https://doi.org/10.1016/0012-821X(91)90215-4.
Mantyla, A.W., Reid, J.L., 1995. On the origins of deep and bottom waters of the Indian Ocean. J. Geophys. Res. Oceans 100, 2417–2439. https://doi.org/10.1029/94JC02564.
McCave, I.N., Kiefer, T., Thornalley, D.J.R., Elderfield, H., 2005. Deep flow in the Madagascar Mascarene Basin over the last 150000 years. Philos. Trans. R. Soc. A Math. Phys. Eng. Sci. 363, 81–99.
McElhinny, M.W., 1970. Formation of the Indian Ocean. Nature 228, 977. https://doi.org/10.1038/228977a0.
McKenzie, D., Sclater, J.G., 1971. The evolution of the Indian Ocean since the late cretaceous. Geophys. J. Int. 24, 437–528. https://doi.org/10.1111/j.1365-246X.1971.tb02190.x.
Miramontes, E., Penven, P., Fierens, R., Droz, L., Toucanne, S., Jorry, S.J., Jouet, G., Pastor, L., Silva Jacinto, R., Gaillot, A., Giraudeau, J., Raisson, F., 2019. The influence of bottom currents on the Zambezi valley morphology (Mozambique Channel, SW Indian Ocean): *in situ* current observations and hydrodynamic modelling. Mar. Geol. 410, 42–55. https://doi.org/10.1016/j.margeo.2019.01.002.
Möller, A., Mezger, K., Schenk, V., 1998. Crustal age domains and the evolution of the continental crust in the Mozambique belt of Tanzania: combined Sm–Nd, Rb–Sr, and Pb–Pb isotopic evidence. J. Petrol. 39, 749–783. https://doi.org/10.1093/petroj/39.4.749.
Mougenot, D., Recq, M., Virlogeux, P., Lepvrier, C., 1986. Seaward extension of the East African Rift. Nature 321, 599. https://doi.org/10.1038/321599a0.
O'Nions, R.K., Carter, S.R., Cohen, R.S., Evensen, N.M., Hamilton, P.J., 1978. Pb, Nd and Sr isotopes in oceanic ferromanganese deposits and ocean floor basalts. Nature 273, 435–438. https://doi.org/10.1038/273435a0.
O'Nions, R.K., Frank, M., von Blanckenburg, F., Ling, H.-F., 1998. Secular variation of Nd and Pb isotopes in ferromanganese crusts from the Atlantic, Indian and Pacific Oceans. Earth Planet. Sci. Lett. 155, 15–28. https://doi.org/10.1016/S0012-821X(97)00207-0.
Olu, K., 2014. PAMELA-MOZ01 cruise. L'Atalante R/V. https://doi.org/10.17600/14001000.
Paquette, J.-L., Nédélec, A., Moine, B., Rakotondrazafy, M., 1994. U-Pb, single zircon Pb-evaporation, and Sm-Nd isotopic study of a granulite domain in SE Madagascar. J. Geol. 102, 523–538. https://doi.org/10.1086/629696.
Pearce, C.R., Jones, M.T., Oelkers, E.H., Pradoux, C., Jeandel, C., 2013. The effect of particulate dissolution on the neodymium (Nd) isotope and rare earth element (REE) composition of seawater. Earth Planet. Sci. Lett. 369–370, 138–147. https://doi.org/10.1016/j.epsl.2013.03.023.
Piepgras, D.J., Jacobsen, S.B., 1988. The isotopic composition of neodymium in the North Pacific. Geochim. Cosmochim. Acta 52, 1373–1381. https://doi.org/10.1016/0016-7037(88)90208-6.
Piepgras, D.J., Wasserburg, G.J., 1980. Neodymium isotopic variations in seawater. Earth Planet. Sci. Lett. 50, 128–138. https://doi.org/10.1016/0012-821X(80)90124-7.
Piepgras, D.J., Wasserburg, G.J., 1982. Isotopic composition of neodymium in waters from the drake passage. Science 217, 207–214.
Piepgras, D.J., Wasserburg, G.J., 1987. Rare earth element transport in the western North Atlantic inferred from Nd isotopic observations. Geochim. Cosmochim. Acta 51, 1257–1271. https://doi.org/10.1016/0016-7037(87)90217-1.
Piepgras, D.J., Wasserburg, G.J., Dasch, E.J., 1979. The isotopic composition of Nd in different ocean masses. Earth Planet. Sci. Lett. 45, 223–236. https://doi.org/10.1016/0012-821X(79)90125-0.
Pin, C., Briot, D., Bassin, C., Poitrasson, F., 1994. Concomitant separation of strontium and samarium-neodymium for isotopic analysis in silicate samples, based on specific extraction chromatography. Anal. Chim. Acta 298, 209–217. https://doi.org/10.1016/0003-2670(94)00274-6.
Piotrowski, A.M., Goldstein, S.L., Hemming, S.R., Fairbanks, R.G., 2004. Intensification and variability of ocean thermohaline circulation through the last deglaciation. Earth Planet. Sci. Lett. 225, 205–220. https://doi.org/10.1016/j.epsl.2004.06.002.
Piotrowski, A.M., Goldstein, S.L., Hemming, S.R., Fairbanks, R.G., 2005. Temporal relationships of carbon cycling and ocean circulation at Glacial boundaries. Science 307, 1933–1938. https://doi.org/10.1126/science.1104883.
Piotrowski, A.M., Banakar, V.K., Scrivner, A.E., Elderfield, H., Galy, A., Dennis, A., 2009. Indian Ocean circulation and productivity during the last glacial cycle. Earth Planet. Sci. Lett. 285, 179–189. https://doi.org/10.1016/j.epsl.2009.06.007.
Piotrowski, A.M., Galy, A., Nicholl, J.A.L., Roberts, N., Wilson, D.J., Clegg, J.A., Yu, J., 2012. Reconstructing deglacial North and South Atlantic deep water sourcing using foraminiferal Nd isotopes. Earth Planet. Sci. Lett. 357–358, 289–297. https://doi.org/10.1016/j.epsl.2012.09.036.
Piper, D.Z., 1974. Rare earth elements in ferromanganese nodules and other marine phases. Geochim. Cosmochim. Acta 38, 1007–1022. https://doi.org/10.1016/0016-7037(74)90002-7.
Quartly, G.D., de Cuevas, B.A., Coward, A.C., 2013. Mozambique Channel eddies in GCMs: a question of resolution and slippage. Ocean Model 63, 56–67. https://doi.org/10.1016/j.ocemod.2012.12.011.
Rahlf, P., Hathorne, E., Laukert, G., Gutjahr, M., Weldeab, S., Frank, M., 2020. Tracing water mass mixing and continental inputs in the southeastern Atlantic Ocean with dissolved neodymium isotopes. Earth Planet. Sci. Lett. 530, 115944. https://doi.org/10.1016/j.epsl.2019.115944.
Rempfer, J., Stocker, T.F., Joos, F., Dutay, J.-C., Siddall, M., 2011. Modelling Nd-isotopes with a coarse resolution ocean circulation model: Sensitivities to model parameters and source/sink distributions. Geochim. Cosmochim. Acta 75, 5927–5950. https://doi.org/10.1016/j.gca.2011.07.044.
Rickli, J., Frank, M., Halliday, A.N., 2009. The hafnium–neodymium isotopic composition of Atlantic seawater. Earth Planet. Sci. Lett. 280, 118–127. https://doi.org/10.1016/j.epsl.2009.01.026.
Rickli, J., Frank, M., Baker, A.R., Aciego, S., de Souza, G., Georg, R.B., Halliday, A.N., 2010. Hafnium and neodymium isotopes in surface waters of the eastern Atlantic Ocean: implications for sources and inputs of trace metals to the ocean. Geochim. Cosmochim. Acta 74, 540–557. https://doi.org/10.1016/j.gca.2009.10.006.
Roberts, N.L., Piotrowski, A.M., McManus, J.F., Keigwin, L.D., 2010. Synchronous deglacial overturning and water mass source changes. Science 327, 75–78. https://doi.org/10.1126/science.1178068.
Rogers, W.E., Hartman, W.D., Krause, K.S.K., 2000. Stratigraphic analysis of upper cretaceous rocks in the Mahajanga Basin, Northwestern Madagascar: implications for ancient and modern faunas. J. Geol. 108, 275–301.
de Ruijter, W.P.M., Ridderinkhof, H., Lutjeharms, J.R.E., Schouten, M.W., Veth, C., 2002. Observations of the flow in the Mozambique Channel: observations in the Mozambique Channel. Geophys. Res. Lett. 29, 140-1–140-3. https://doi.org/10.1029/2001GL013714.
Rutberg, R.L., Hemming, S.R., Goldstein, S.L., 2000. Reduced North Atlantic Deep Water flux to the glacial Southern Ocean inferred from neodymium isotope ratios. Nature 405, 935. https://doi.org/10.1038/35016049.
Schacht, U., Wallmann, K., Kutterolf, S., 2010. The influence of volcanic ash alteration on the REE composition of marine pore waters. J. Geochem. Explor. 106, 176–187. https://doi.org/10.1016/j.gexplo.2010.02.006. GEOFLUIDS VI: Recent Advances in Research on Fluids in Geological Processes.
Schott, F.A., McCreary, J.P., 2001. The monsoon circulation of the Indian Ocean. Prog. Oceanogr. 51, 1–123. https://doi.org/10.1016/S0079-6611(01)00083-0.
Segl, M., Mangini, A., Bonani, G., Hofmann, H.J., Nessi, M., Suter, M., Wölfli, W., Friedrich, G., Plüger, W.L., Wiechowski, A., Beer, J., 1984. 10 Be-dating of a manganese crust from Central North Pacific and implications for ocean palaeocirculation. Nature 309, 540. https://doi.org/10.1038/309540a0.
Shimizu, H., Tachikawa, K., Masuda, A., Nozaki, Y., 1994. Cerium and neodymium isotope ratios and REE patterns in seawater from the North Pacific Ocean. Geochim. Cosmochim. Acta 58, 323–333. https://doi.org/10.1016/0016-7037(94)90467-7.
Stichel, T., Frank, M., Rickli, J., Hathorne, E.C., Haley, B.A., Jeandel, C., Pradoux, C., 2012b. Sources and input mechanisms of hafnium and neodymium in surface waters of the Atlantic sector of the Southern Ocean. Geochim. Cosmochim. Acta 94, 22–37. https://doi.org/10.1016/j.gca.2012.07.005.
Storey, M., Mahoney, J.J., Saunders, A.D., Duncan, R.A., Kelley, S.P., Coffin, M.F., 1995. Timing of hot spot—related volcanism and the breakup of Madagascar and India. Science 267, 852–855. https://doi.org/10.1126/science.267.5199.852.
Tachikawa, K., Handel, C., Dupré, B., 1997. Distribution of rare earth elements and neodymium isotopes in settling particulate material of the tropical Atlantic Ocean (EUMELI site). Deep Sea Res. Part Oceanogr. Res. Pap. 44, 1769–1792. https://doi.org/10.1016/S0967-0637(97)00057-5.
Tachikawa, K., Athias, V., Jeandel, C., 2003. Neodymium budget in the modern ocean and paleo-oceanographic implications. J. Geophys. Res. Oceans 108. https://doi.org/10.1029/1999JC000285.
Tachikawa, K., Arsouze, T., Bayon, G., Bory, A., Colin, C., Dutay, J.-C., Frank, N., Giraud, X., Gourlan, A.T., Jeandel, C., Lacan, F., Meynadier, L., Montagna, P., Piotrowski, A.M., Plancherel, Y., Pucéat, E., Roy-Barman, M., Waelbroeck, C., 2017. The large-scale evolution of neodymium isotopic composition in the global modern and Holocene ocean revealed from seawater and archive data. Chem. Geol. 457, 131–148. https://doi.org/10.1016/j.chemgeo.2017.03.018.
Tanaka, T., Togashi, S., Kamioka, H., Amakawa, H., Kagami, H., Hamamoto, T., Yuhara, M., Orihashi, Y., Yoneda, S., Shimizu, H., Kunimaru, T., Takahashi, K., Yanagi, T., Nakano, T., Fujimaki, H., Shinjo, R., Asahara, Y., Tanimizu, M., Dragusanu, C., 2000. JNdi-1: a neodymium isotopic reference in consistency with LaJolla neodymium. Chem. Geol. 168, 279–281. https://doi.org/10.1016/S0009-2541(00)00198-4.
Thompson, J.O., Moulin, M., Aslanian, D., de Clarens, P., Guillocheau, F., 2019. New starting point for the Indian Ocean: second phase of breakup for Gondwana. Earth-Sci. Rev. 191, 26–56. https://doi.org/10.1016/j.earscirev.2019.01.018.

Toole, J.M., Warren, B.A., 1993. A hydrographic section across the subtropical South Indian Ocean. Deep Sea Res. Part Oceanogr. Res. Pap. 40, 1973–2019. https://doi.org/10.1016/0967-0637(93)90042-2.

Torsvik, T.H., Tucker, R.D., Ashwal, L.D., Carter, L.M., Jamtveit, B., Vidyadharan, K.T., Venkataramana, P., 2000. Late Cretaceous India-Madagascar fit and timing of break-up related magmatism. Terra Nova 12, 220–224. https://doi.org/10.1046/j.1365-3121.2000.00300.x.

Ullgren, J.E., van Aken, H.M., Ridderinkhof, H., de Ruijter, W.P.M., 2012. The hydrography of the Mozambique Channel from six years of continuous temperature, salinity, and velocity observations. Deep Sea Res. Part Oceanogr. Res. Pap. 69, 36–50. https://doi.org/10.1016/j.dsr.2012.07.003.

Wei, R., Abouchami, W., Zahn, R., Masque, P., 2016. Deep circulation changes in the South Atlantic since the Last Glacial Maximum from Nd isotope and multi-proxy records. Earth Planet. Sci. Lett. 434, 18–29. https://doi.org/10.1016/j.epsl.2015.11.001.

Weijer, W., 1999. Impact of interbasin exchange on the Atlantic overturning circulation. J. Phys. Oceanogr. 29, 19.

Wilson, D.J., Piotrowski, A.M., Galy, A., McCave, I.N., 2012. A boundary exchange influence on deglacial neodymium isotope records from the deep western Indian Ocean. Earth Planet. Sci. Lett. 341–344, 35–47. https://doi.org/10.1016/j.epsl.2012.06.009.

You, Y., 2000. Implications of the deep circulation and ventilation of the Indian Ocean on the renewal mechanism of North Atlantic Deep Water. J. Geophys. Res. Oceans 105, 23895–23926. https://doi.org/10.1029/2000JC900105.

Yu, J., Elderfield, H., Piotrowski, A.M., 2008. Seawater carbonate ion-δ13C systematics and application to glacial–interglacial North Atlantic ocean circulation. Earth Planet. Sci. Lett. 271, 209–220. https://doi.org/10.1016/j.epsl.2008.04.010.